



A Journal of



Accepted Article

Title: Heterobimetallic Pt(II)–Au(I) Complexes Comprising Unsymmetrical 1,1-Bis(diphenylphosphino)methane Bridge: Synthesis, Photophysical and Cytotoxic Studies

Authors: Hamid R. Shahsavari, Nora Giménez, Elena Lalinde, M. Teresa Moreno, Masood Fereidoonnehad, Reza Babadi Aghakhanpour, Mehri Khatami, Foroogh Kalantari, Zahra Jamshidi, and Mozhdeh Mohammadpour

This manuscript has been accepted after peer review and appears as an Accepted Article online prior to editing, proofing, and formal publication of the final Version of Record (VoR). This work is currently citable by using the Digital Object Identifier (DOI) given below. The VoR will be published online in Early View as soon as possible and may be different to this Accepted Article as a result of editing. Readers should obtain the VoR from the journal website shown below when it is published to ensure accuracy of information. The authors are responsible for the content of this Accepted Article.

To be cited as: *Eur. J. Inorg. Chem.* 10.1002/ejic.201801297

Link to VoR: <http://dx.doi.org/10.1002/ejic.201801297>

WILEY-VCH

Heterobimetallic Pt(II)–Au(I) Complexes Comprising Unsymmetrical 1,1-Bis(diphenylphosphino)methane Bridge: Synthesis, Photophysical and Cytotoxic Studies

Hamid R. Shahsavari*^[a], Nora Giménez^[b], Elena Lalinde*^[b], M. Teresa Moreno^[b], Masood Fereidoonzhad*^[c,d], Reza Babadi Aghakhanpour^[a], Mehri Khatami^[a], Foroogh Kalantari^[d], Zahra Jamshidi^[e], and Mozhddeh Mohammadpour^[e]

Abstract: In the present work, a series of aryl-cycloplatinated(II) complexes with general formula $[\text{Pt}(\text{C}^{\wedge}\text{N})(\text{Ar})(\kappa^1\text{-dppm})]$, **1**, [$\text{C}^{\wedge}\text{N}$ = 7,8-benzoquinolinyl (bzq) or 2-phenylpyridinyl (ppy); Ar = C_6F_5 or *p*-MeC₆H₄, dppm = 1,1-bis(diphenylphosphino)methane] were employed in the reaction with AuCl(SMe₂) in order to generate heterobimetallic Pt(II)-Au(I) complexes, $[\text{Pt}(\text{C}^{\wedge}\text{N})(\text{Ar})(\mu\text{-dppm})\text{Au}(\text{Cl})]$, **2**, featuring a dppm bridge between the metal centers. The expectation was to induce metallophilic character into the excited state and to reduce non-radiative deactivation pathways of the dangling auxiliary $\kappa^1\text{-dppm}$ ligand through molecular motions, to improve the photophysical properties. After characterization of the new complexes by means of NMR spectroscopy and X-ray crystallography technique, the photophysical properties of all the complexes were investigated by UV-Vis and photoluminescence spectroscopies. Both of the monometallic complexes and heterobimetallic products have shown to be luminescent in different states and temperature conditions. However, by addition of Au(I), the impact on the photophysics of the heterobimetallic products in relation to the precursors with dangling dppm is minimal, a finding which can be attributed to the absence of a Pt(II)-Au(I) bond in these compounds. Indeed, the character of the excited states of the monomer Pt(II) complexes and their corresponding bimetallic Pt(II)-Au(I) ones are similar, as confirmed by density functional theory (DFT) and time resolved DFT (TD-DFT) calculations. The cytotoxic activities of the compounds along with that of $[\text{ClAu}(\mu\text{-dppm})\text{AuCl}]$ were evaluated

against human breast cancer (MCF-7), human lung cancer (A549), human ovarian cancer (SKOV3) and non-tumorigenic epithelial breast (MCF-10A) cell lines. The highest activity was found for the heterometallic Pt-Au species, suggesting a cooperative effect of both metallic fragments. The most cytotoxic compound, *i.e.* $[\text{Pt}(\text{bzq})(p\text{-MeC}_6\text{H}_4)(\mu\text{-dppm})\text{Au}(\text{Cl})]$, **2b**, effectively causes cell death in MCF-7 cancer cell line by inducing apoptosis. Fluorescence microscopy experiments for **2a** were performed.

Introduction

The rational design and synthesis of mixed metal complexes have been a rising area of interest in recent years.^[1] For example, mixed metal complexes have been successfully applied in catalysis of sequential reactions in which each metal center was found to play the role of one catalytic center,^[2] and, in many occasions, the heterometallic complexes exhibited a higher catalytic activity or selectivity compared with their monometallic analogues.^[3] Furthermore, the combination of two or more metal centers into a unique structure have been shown to enhance the anticancer activity of the structure or to induce unique properties due to the new physicochemical characteristics, coming from synergic effects between the metal centers.^[4] Sometimes, these complexes display luminescent properties due to presence of organic luminophores in their structure, what provides the possibility to be visualized by fluorescence microscopy. In this context, luminescent heterometallic complexes provide the opportunity to generate new metal-based structures able of displaying cytotoxic activity and give information about their internalization mechanism, localization, biodistribution and biological targets.^[4b, 5]

The metal centers can be linked by variable spacer ligands in order to form heterobimetallic complexes; however, no diversity is observed in these ligands to be appropriate candidates as spacers mainly due to the difficulty in prohibiting the formation of undesirable chelate instead of an appropriate bridging ligand or reorganization processes leading to symmetrical homobimetallic systems.^[5c] Among the linker ligands, 1,1-bis(diphenylphosphino)methane (dppm) has a special dignity for two reasons. First, dppm in its chelated form is under strain due to the formation of four-membered ring and, this fact facilitates the binding coordination mode as monodentate ligand with a free phosphine head. Secondly, due to the presence of a short chain between the phosphine heads, dppm is able to hold the metal centers close to each other in which the formation of metal-metal

[a] Dr. H. R. Shahsavari, Dr. R. Babadi Aghakhanpour, M. Khatami; Department of Chemistry, Institute for Advanced Studies in Basic Sciences (IASBS), Zanjan 45137-66731, Iran. E-mail: shahsavari@iasbs.ac.ir
<https://iasbs.ac.ir/personalpage?id=32125&staff=0>

ORCID: 0000-0002-2579-2185

[b] Nora Giménez, Prof. Elena Lalinde, Prof. M. Teresa Moreno; Departamento de Química-Centro de Síntesis Química de La Rioja, (CISQ), Universidad de La Rioja, 26006, Logroño, Spain. E-mail: elena.lalinde@unirioja.es
<https://cisq.unirioja.es/en/gmmo.php>

[c] Dr. M. Fereidoonzhad; Toxicology Research Center, Ahvaz Jundishapur University of Medical Sciences, Ahvaz, Iran. E-mail: fereidoonzhad-m@ajums.ac.ir
http://isid.research.ac.ir/Masood_Fereidoonzhad

[d] Dr. M. Fereidoonzhad, Foroogh Kalantari; Department of Medicinal Chemistry, Student Research Committee, Ahvaz Jundishapur University of Medical Sciences, Ahvaz, Iran.

[e] Dr. Z. Jamshidi, Dr. M. Mohammadpour; Chemistry & Chemical Engineering Research Center of Iran, Tehran, 14968-13151, Iran.

Supporting information for this article is given via a link at the end of the document.

FULL PAPER

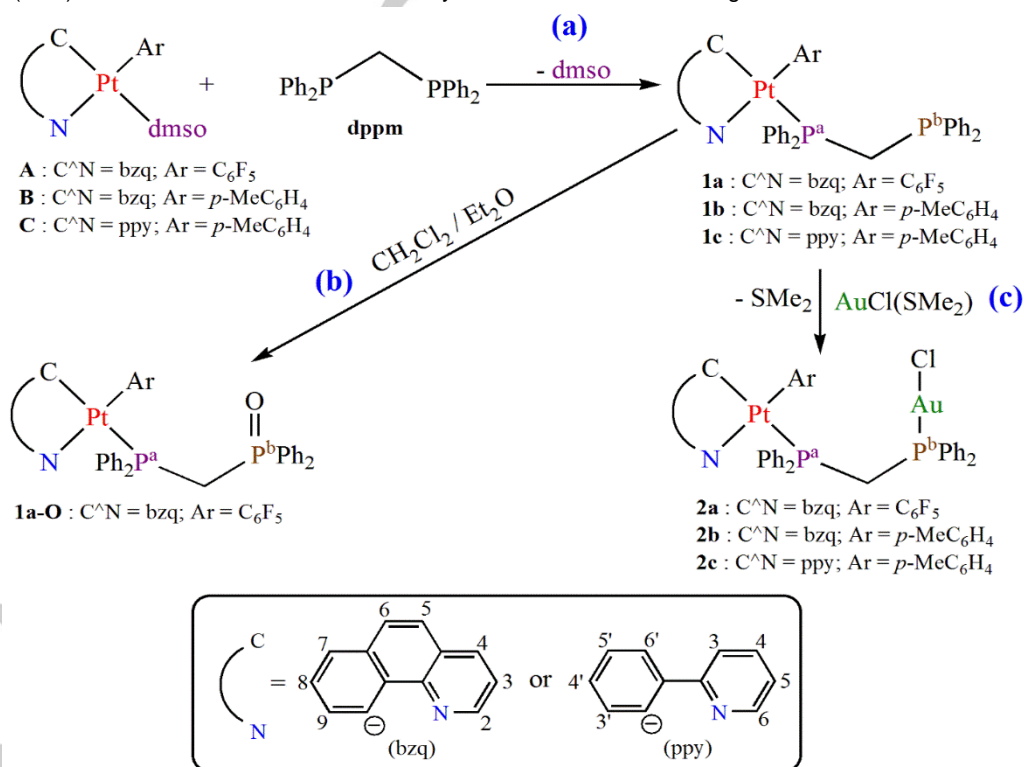
bond becomes more probable. These properties of the dpmm make it a good candidate to be located as an unsymmetrical bridge between two different metal centers particularly in d^8 - d^{10} or d^8 - d^8 heterobimetallic complexes. In the synthesis of such complexes, firstly, a complex featuring one (or more) monodentate κ^1 -dpmm ligand is isolated and then reacted with the second metal center to generate a heterobinuclear structure. It is worthy to note that some of these heterometallic complexes, in occasions, exhibit luminescence properties, which have been associated to the presence of metal-metal bonds.^[6]

Cycloplatinated(II) complexes are an important class of compounds because of their attractive photochemical and photophysical properties with successful applications in light emitting devices,^[7] dye sensitized solar cell,^[8] biosensors, photo-switches,^[9] optoelectronic devices,^[10] photocatalysts^[11] and biological imaging.^[12] These complexes display very strong Pt-C bonds that increase the energy of the higher lying metal-centered d - d states to a level high enough to suppress the thermal population. Consequently, depending on the auxiliary ligand, these complexes display highly efficient and tunable phosphorescence attributed to 3 LC or admixtures 3 LC/ 3 MLCT or 3 LLCT/ 3 MLCT states.^[10a, 13] Heteronuclear cycloplatinated complexes with the metal centers connected via metallophilic interactions,^[14] or remotely connected through a linker ligand^[15] are also an intensively studied research area, mainly due to their interesting luminescence properties, though in these systems a straight relationship between structures and emission properties is still unclear.

In recent years, cycloplatinated(II) complexes have also attracted growing attention for their possible use as anticancer drugs and the results are quite promising.^[16] These complexes, possess strong σ (Pt-C) bonds what increases their stability in

physiological conditions, avoiding off-target reactions, and, therefore, simplifies the potential therapeutic applications.^[17] Additionally, recent studies have also demonstrated that the antiproliferative properties of some of these platinum complexes improved upon attaching a second Au(I) unit to the organometallic Pt compound.^[18] Because of the mechanisms of action of gold complexes are likely to be different from those of platinum, in some cases, the heteronuclear Pt(II)-Au(I) complexes exhibit antiproliferative properties *in vitro* in human cancer cells in the range of cisplatin or higher.^[14c, 15]

Following our interest on cycloplatinated complexes featuring an unsymmetrical dpmm bridge,^[19] in this contribution some [Pt(C[^]N)(Ar)(κ^1 -dpmm)], **1**, complexes with monodentate dpmm ligand were employed as precursors to give a series of heterobimetallic complexes with general formula [Pt(C[^]N)(Ar)(μ -dpmm)AuCl], **2**. We anticipated that an *intra*-molecular metallophilic interaction could be established between Pt(II) and Au(I) centers, which could influence the optical properties.^[14b] In addition, it is worthy to note that among the new non-platinum drugs especially gold compounds have gained more attention.^[20] Epidemiological, clinical and experimental studies show that gold metallodrugs are promising cancer chemotherapeutic agents.^[21] Auranofin, one of the best-known lead structure of gold(I) complexes, which also incorporates a phosphine ligand, is under phase I/II clinical trial studies for the treatment of non-small cell lung cancer,^[22] small cell lung cancer,^[22] ovarian cancer,^[23] and primary peritoneal cancer.^[23] In this context, complexes **1** and **2** offer us the opportunity to investigate the role of the two metallic fragments in the cytotoxic activity and properties of the final complexes. A number of reports support the idea that bimetallic complexes may enable novel and synergic modes of interaction with biomolecular targets.^[24]



Scheme 1. Synthetic routes for (a) Pt(II)-dpmm, (b) Pt(II)-dpmmO and (c) Pt(II)-Au(I) complexes, with atom numbering of the C[^]N ligands.

FULL PAPER

Results and Discussion

Synthesis and Characterization

The syntheses of the platinum complexes and the heterobimetallic Pt-Au complexes was carried out as depicted in Scheme 1. Treatment of the heteroleptic aryl-cycloplatinated complexes $[\text{Pt}(\text{C}^{\wedge}\text{N})(\text{Ar})(\text{dmsO})]$ (**A-C**)^{66, 67} with 1,1-bis(diphenylphosphino)methane (dppm) in acetone, in a 1:1 molar ratio, provided yellow or greenish solutions, which after workup afforded the corresponding monodentate complexes $[\text{Pt}(\text{C}^{\wedge}\text{N})(\text{Ar})(\kappa^1\text{-dppm})]$, **1**, Ar = C₆F₅, C[^]N = bzq (**1a**); Ar = *p*-MeC₆H₄, C[^]N = bzq (**1b**);^[19a] Ar = *p*-MeC₆H₄, C[^]N = ppy (**1c**),^[19a]

respectively, in which, the dppm ligand behaves as a monodentate pendant ligand. It should be noted, that the synthesis and characterization of tolyl complexes, **1b** and **1c**, has been previously reported.^[19a] The pentafluorophenyl complex, **1a**, is new and it was characterized by different spectroscopic methods. It was found that the free phosphine head is oxidized during the crystallization process in the solvent mixture of CH₂Cl₂/Et₂O, yielding the complex $[\text{Pt}(\text{bzq})(\text{C}_6\text{F}_5)(\kappa^1\text{-dppmO})]$, **1aO**. Finally, the complexes **1a-c** were reacted with the Au precursor complex $[\text{AuCl}(\text{SMe}_2)]$ ^[26] to give the new heterobimetallic complexes $[\text{Pt}(\text{C}^{\wedge}\text{N})(\text{Ar})(\mu\text{-dppm})\text{AuCl}]$, **2**, Ar = C₆F₅, C[^]N = bzq (**2a**); Ar = *p*-MeC₆H₄, C[^]N = bzq (**2b**); Ar = *p*-MeC₆H₄, C[^]N = ppy (**2c**), respectively.

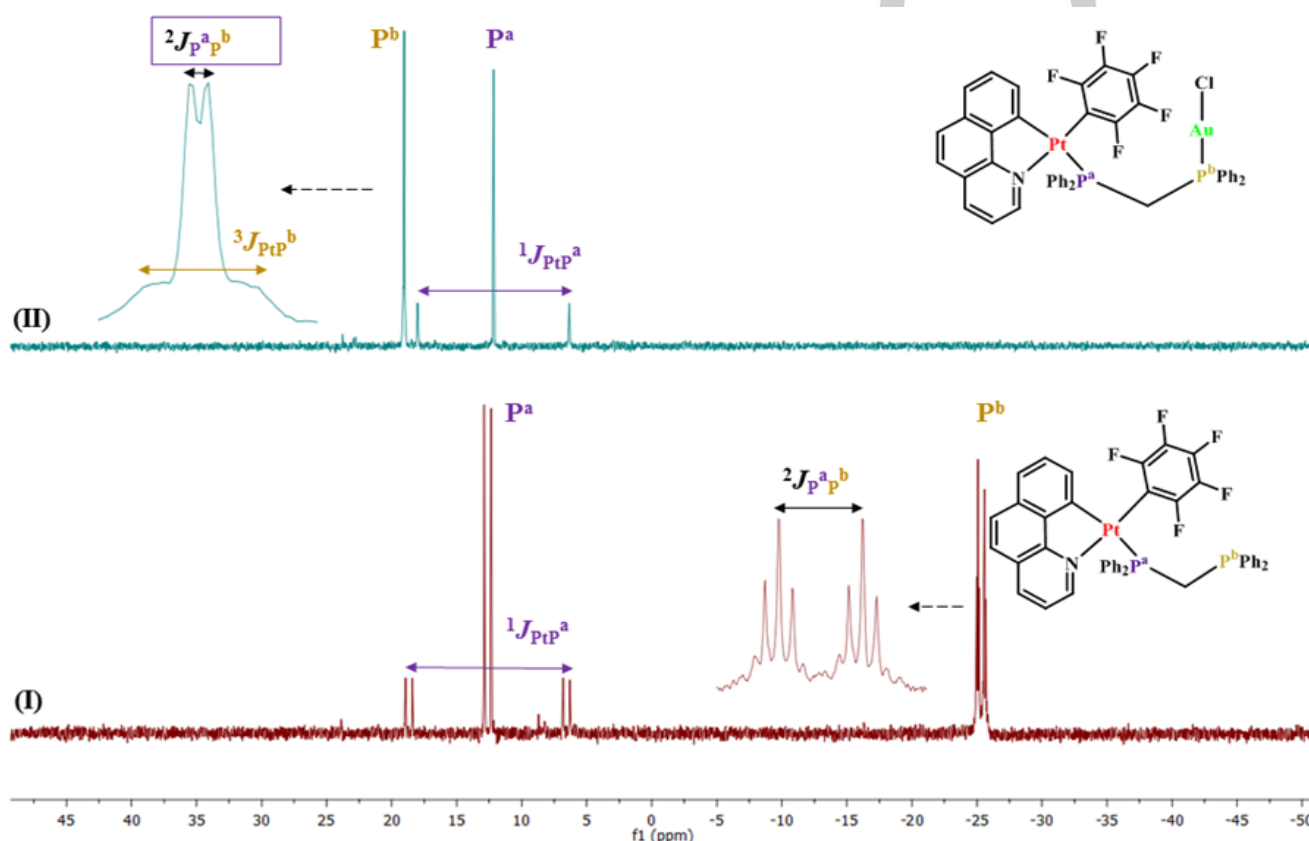


Figure 1. $^{31}\text{P}\{^1\text{H}\}$ NMR spectra of the complexes I) **1a**, and II) **2a**.

The new complexes **1a**, **2a-c** were analyzed by ESI (electrospray ionization) mass spectroscopy and characterized by multinuclear (^1H , $^{31}\text{P}\{^1\text{H}\}$, ^{19}F) NMR spectroscopy. The corresponding ESI (+) mass spectra of the complexes **1a**, **2a**, **2b** and **2c** are related to $[\text{M}-\text{C}_6\text{F}_5]^+$, $[\text{M} + \text{Na}]^+$ and $[\text{M} + \text{H}]^+$ fragments, respectively. The numerical details for the NMR spectra are listed in the Experimental Section. The ^{19}F NMR spectra of **1a** and **1aO** exhibit the typical AA'MXX' pattern for 2-*o*-F, *p*-F and 2-*m*-F of the C₆F₅ ring with relatively high $^3J_{^{19}\text{F}-^{31}\text{P}}$ (496 Hz **1a**, 490 Hz **1aO**), supporting the *trans* disposition of the N relative to the pentafluorophenyl group. As illustration, the $^{31}\text{P}\{^1\text{H}\}$ NMR spectra of complexes **1a/2a** and **1c/2c** are provided in Figures 1 and S5, respectively. The $^{31}\text{P}\{^1\text{H}\}$ NMR spectrum of **1a** (see Figure 1) compares to those of related **1b,c**. It displays the expected two different signals due to the coordinated (δ P^a 12.62) and free (δ P^b -25.3) P atoms of dppm, respectively, The low field

resonance, P^a appears as doublet ($^2J_{\text{P}^{\text{a}}\text{P}^{\text{b}}} = 13$ Hz) and exhibits one-bond Pt coupling constant of 1963 Hz, comparable to those found in **1b,c**, whereas P^b is resolved as pseudo-triplet due to the additional coupling to a close *o*-F of C₆F₅ group. For **1aO**, the oxidation of the terminal phosphorus atom causes a remarkable downfield shift of the P^b signal (δ 25.3) and a slight increase of the three bond $^{195}\text{Pt}-^{31}\text{P}^{\text{b}}$ coupling constant (46 Hz). For all the heterobimetallic complexes **2a-c**, the most significant feature is observed in the P^b resonance, which also shifts downfield, in relation to the precursors, due to coordination to Au(I), whereas, interestingly, the $^1J_{\text{PtP}^{\text{a}}}$ value is slightly reduced (1890 **2a**; 2032 **2b**, 1960 Hz **2c** vs 1963 **1a**; 2082 **1b**, 2015 Hz **1c**).

The structures of complexes **1aO**, **2a** and **2b** were established by X-ray crystallography (details in the Supporting Information). Although complex **1a** is completely stable in the solid state, crystals of **1aO** in which the free P head of dppm is oxidized, were separated during attempts to obtain nanocrystals suitable

FULL PAPER

for X-ray for complex **1a** in $\text{CH}_2\text{Cl}_2/\text{Et}_2\text{O}$. Figure 2 shows the ORTEP plot of the complex **1aO** and a selection of corresponding geometrical parameters is given in Table S1. The structure confirms the square-planar coordination environment for the Pt(II) atom, whose bond distances and angles were similar to other related cyclometalated derivatives,^[26] as well as the mutually *trans* disposition between the nitrogen (N1) atom of the bzq ligand and the ipso-C (C14) of the C_6F_5 group. The P2-O1 bond length [1.484(2) Å] and the O1–P2–C angles [112.7(1)–113.5(1)°] of the terminal dppm-O ligand are in the range of those observed for terminal phosphine oxides.^[27] The P2–C44–P1 backbone of the

dppm-O ligand is inclined by 63.13° to the Pt coordination, locating the oxygen atom far away the platinum center [Pt...O 4.858(2) Å]. It is noteworthy that one of the phenyl groups lies above the cycloplatinated ring close to the Pt atom with a Pt–C43 distance [3.472(4) Å] shorter than the Van der Waals limit (4.09 Å),^[28] suggesting some degree of Pt... π (phenyl) interaction. As is typical in this type of complexes, the crystal packing of **1aO** includes extensive intermolecular $\pi\cdots\pi$ [bzq...bzq (C...C 3.398 Å) interactions and weak [O...H (2.618 Å), F...H (2.564 Å)] contacts (Figure S6).

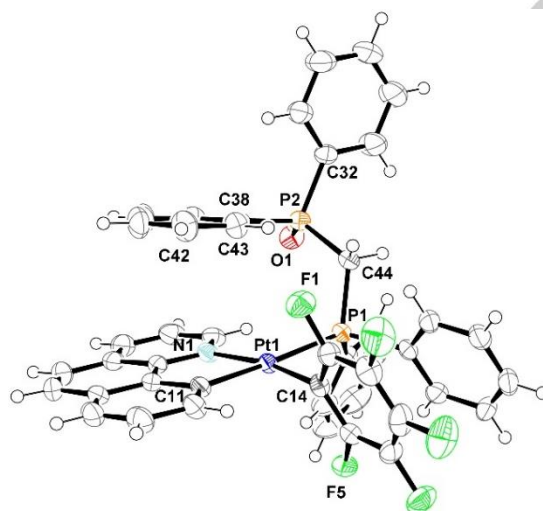


Figure 2. ORTEP view of **1aO**. Ellipsoids are drawn at the 50% probability level.

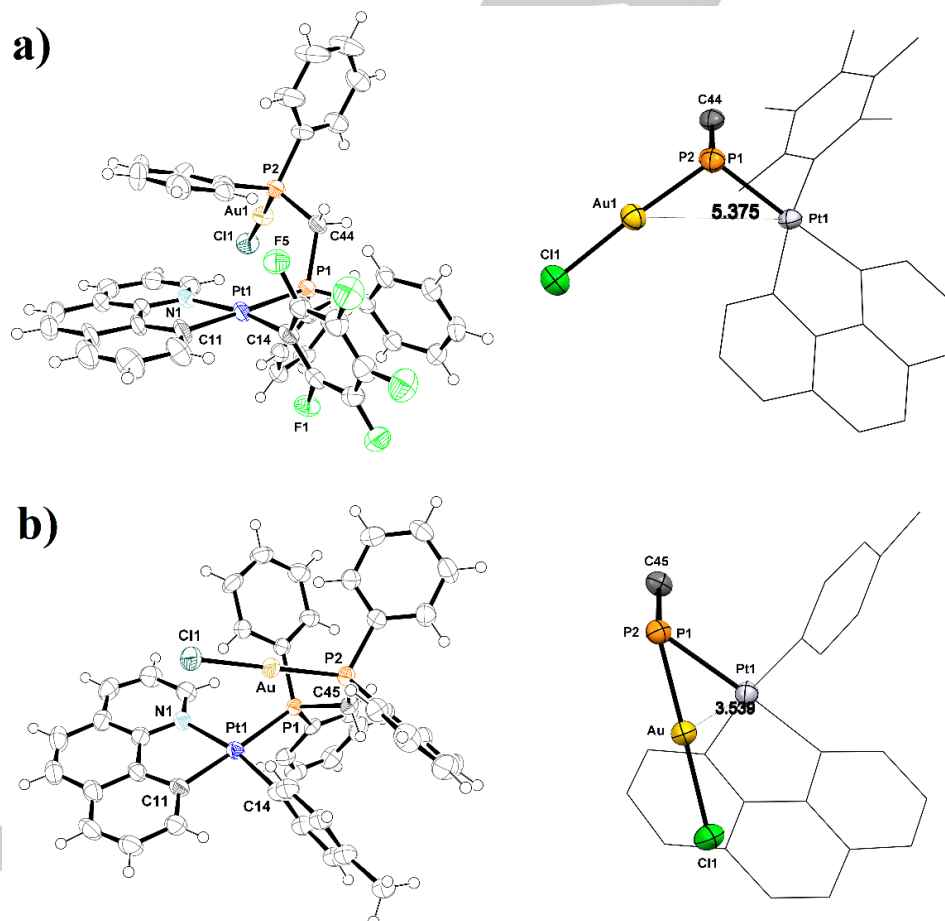


Figure 3. ORTEP views of **2a** and **2b**. Ellipsoids are drawn at the 50% probability level.

FULL PAPER

Views of the crystal structures of the complexes **2a** and **2b** are given in Figure 3 and a selection of the bond lengths and angles are also included in Table S1. The crystal structures confirm the coordination of the AuCl unit to the P of the dpmp ligand of the precursors, which acts as a bringing group between the Pt chromophore and the Au center. The type of ancillary ligand, *i.e.* C₆F₅ (**2a**) or MeC₆H₄ (**2b**), considerably affects the orientation of P-Au-Cl moiety in relation to the square planar Pt(II) moiety. In **2a**, and likely due to steric constraints of the bulky C₆F₅ ligand, the planar Pt(II) and P-Au-Cl moieties are situated in the opposite sides in relation to each other, whereas, in the case of **2b**, the Au-Cl unit leans towards the Pt center. As a consequence the Au-Pt distance in **2a** (5.375 Å) is remarkably longer than that observed

for **2b** (3.539 Å). This later distance is larger than those found in complexes [Pt(bzq)Me(*μ*-dppy)AuCl] [2.9850(4) Å]^[14h] and ([Pt(*κ*²-2-C₆X₄PPh₂)(PPh₃)(*μ*-2-C₆X₄PPh₂)AuCl] [X = H 3.3902(2), X = F 3.1459(2) Å]^[29] and longer than the sum of the van der Waals radii of the two metals (3.41 Å)^[28] excluding metallophilic interactions.

The crystal packing of **2a** (Figure S7) contains dimers supported by intermolecular $\pi \cdots \pi$ contacts (bzq \cdots bzq 3.268–3.333 Å) (pink lines), reinforced by H_{Ph} \cdots Cl (2.744–2.882 Å), H_{Ph} \cdots F_{C6F5} (2.550 Å), H_{Ph} \cdots C_{Ph} and H_{Ph} \cdots C_{bzq} (2.784–2.875 Å) secondary interactions (blue lines), whereas **2b** shows a supra-molecular packing, being supported by H_{Ph} \cdots C_{bzq} (2.761–2.838 Å) and Cl \cdots H_{bzq} (2.764–2.788 Å) short interactions (Figure S8).

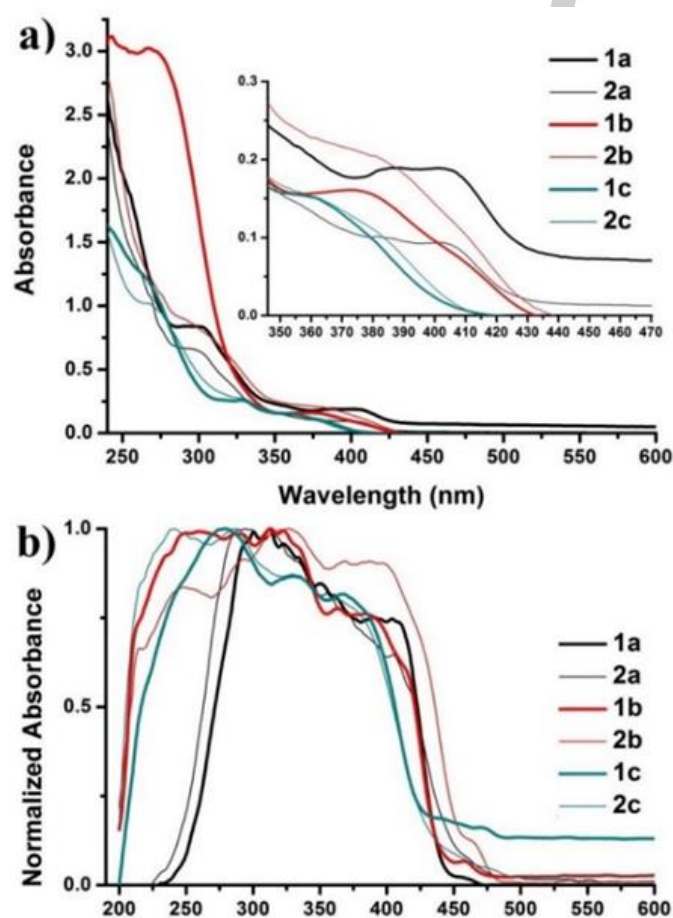


Figure 4. a) UV-Vis absorbance spectra of **1-2a**, **1-2b** and **1-2c** in CH₂Cl₂ solutions (5×10⁻⁵ M). b) DRUV (diffuse reflectance UV-Vis) spectra of **1-2a**, **1-2b** and **1-2c**.

UV-Vis spectra

The electronic absorption spectra of all complexes recorded in dilute CH₂Cl₂ solutions are displayed in Figure 4a, while the relevant data are summarized in Table S2. The high energy intense bands with wavelengths below 325 nm can be attributed to π - π^* intra-ligand ¹IL or ¹IL' transitions mainly centered on the cyclometalated ligand [L = bzq or ppy] and L' = aryl groups [C₆F₅ or *p*-MeC₆H₄]. In addition to the mentioned transitions, these bands have also contributions from intra-ligand charge transfer in the phenyl rings of dpmp. With reference to previous assignments in related complexes,^[1a] the low energy absorption bands above 325 nm could be attributed to mixed ¹MLCT/¹IL transitions, with some ¹L'LCT contribution in the tolyl derivatives as suggested by theoretical calculations. The ¹MLCT transitions can involve

charge transfer from Pt(II) to cyclometalated, and phosphine ligands in complexes **1** and, additionally, from Au(I) to phosphine ligand in complexes **2**. Expectedly, the bands for bzq complexes (**a,b**) are red-shifted in relation to those of ppy complexes, being attributed to the extending π -conjugation system in bzq ligand.^[30] As can be seen in Figure 4, the spectra of the heterometallic Pt(II)-Au(I) complexes (**2a-c**) are rather similar to their corresponding precursors (**1a-c**) not only in CH₂Cl₂ solution but also in the solid state (Figure 4b).

FULL PAPER

Table 1. Emission parameters for 1a-c and 2a-c.

| Complex | State (Temp.) | λ_{em}/nm^a | $\tau/\mu s$ | $\Phi(\%)$ |
|---------|--|---|------------------------|------------|
| 1a | Solid (298 K) | 492 ^{max} , 519, 558 ^{sh} | 8.4 (89%), 24.1 (11%) | 3 |
| | Solid (77 K) | 494 ^{max} , 530, 570 ^{sh} | 532 (53%), 311 (47%) | |
| | CH ₂ Cl ₂ 5×10 ⁻⁵ M (77 K) | 478 ^{max} , 514, 553 ^{sh} | | |
| 1b | Solid (298 K) | 485 ^{max} , 520, 565 ^{sh} | 30.4 | 11 |
| | Solid (77 K) | 485 ^{max} , 521, 564 ^{sh} | 221.1(68%), 68.2 (32%) | |
| | CH ₂ Cl ₂ 5×10 ⁻⁵ M (77 K) | 484 ^{max} , 519, 555 ^{sh} | | |
| 1c | Solid (298 K) | 476 ^{max} , 509, 538 ^{sh} | 11.7 | 95 |
| | Solid (77 K) | 474 ^{max} , 508, 538 ^{sh} | 72.3 | |
| | CH ₂ Cl ₂ 5×10 ⁻⁵ M (77 K) | 480 ^{max} , 511, 545 ^{sh} | | |
| 2a | Solid (298 K) | 494 ^{max} , 524 | 10.44 | 2 |
| | Solid (77 K) | 494 ^{max} , 533, 571 ^{sh} | 380 | |
| | CH ₂ Cl ₂ 5×10 ⁻⁵ M (298 K) | 465 ^{max} , 496, 520 ^{sh} | 0.3 | |
| | CH ₂ Cl ₂ 5×10 ⁻⁵ M (77 K) | 478 ^{max} , 513, 553 ^{sh} | | |
| 2b | Solid (298 K) | 491 ^{max} , 526, 574 ^{sh} | 32.9 | 29.3 |
| | Solid (77 K) | 494 ^{max} , 528, 568 ^{sh} | 89.4 | |
| | CH ₂ Cl ₂ 5×10 ⁻⁵ M (77 K) | 485 ^{max} , 521, 558 ^{sh} | | |
| 2c | Solid (298 K) | 495, 515 ^{max} , 554 ^{sh} | 9.6 | 3.7 |
| | Solid (77 K) | 489 ^{max} , 524, 564 ^{sh} | 56.2 | |
| | CH ₂ Cl ₂ 5×10 ⁻⁵ M (77 K) | 478 ^{max} , 514, 542 ^{sh} | | |

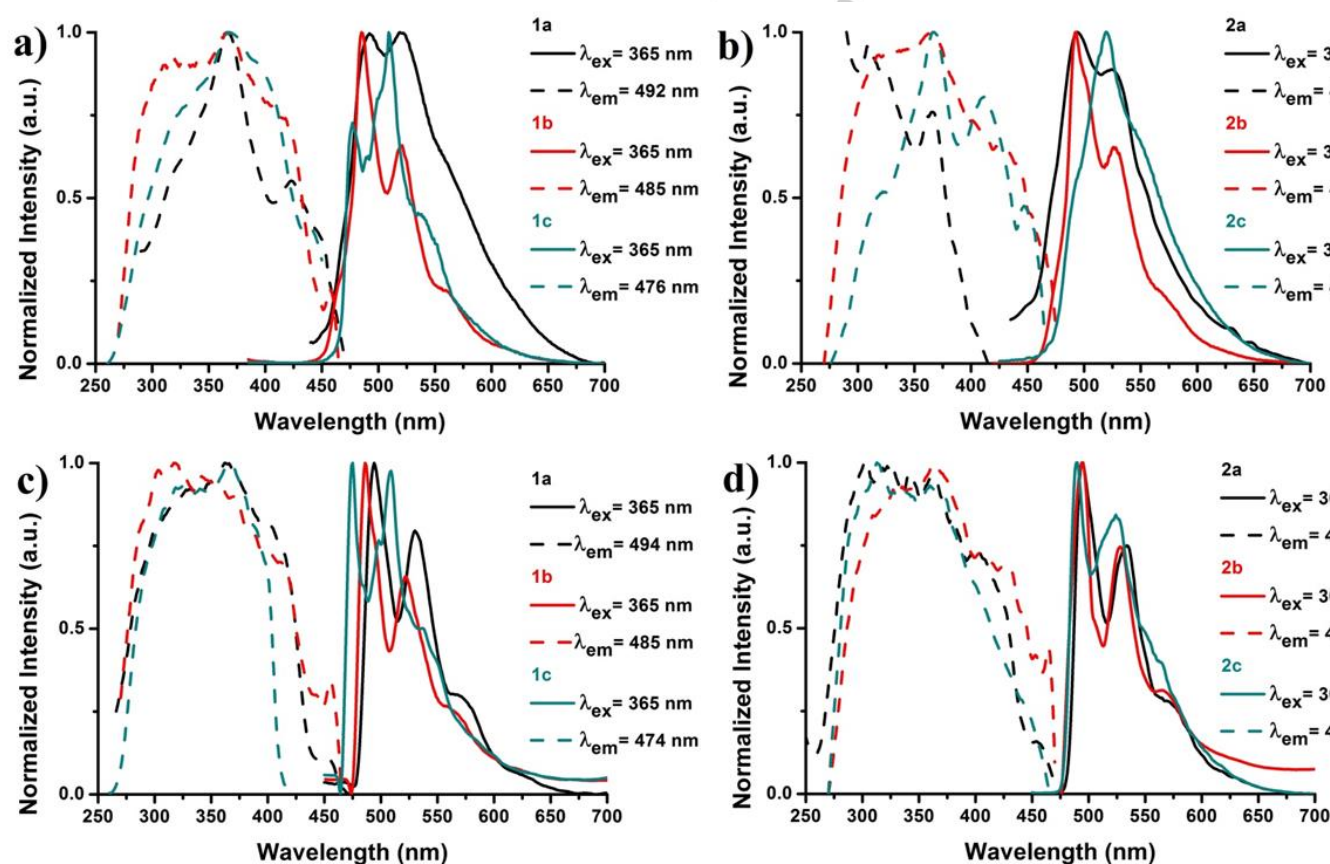
^a λ_{exc} 365-380 nm.

Figure 5. Normalized emission (solid lines) and excitation (dashed lines) spectra in the solid state of a) 1a-c at 298 K, b) 2a-c at 298 K, c) 1a-c at 77 K and d) 2a-c at 77 K.

Photoluminescence Spectra

All complexes (1a-c, 2a-c) exhibit emission in the green region, in rigid media, either in the solid state (298, 77 K) or in a CH₂Cl₂ glassy matrix at 77 K. Excluding complex 2a, the rest of complexes are not luminescent in fluid CH₂Cl₂ solution. The

remarkable quenching of the emission in fluid solution could be ascribed to ease non-radiative deactivation through molecular motions and non-covalent intermolecular interactions enhanced in the monodentate κ^1 -dppm precursors 1, due to the presence of the dangling free phosphine. Besides, ease thermal access to

FULL PAPER

non-emissive metal centered $d-d$ excited states and also direct solvent interactions should not be ruled out.^[17a, 31]

The luminescence spectra obtained in solid at 298 K and at 77K are reported in Figure 5 and those obtained in CH_2Cl_2 at 77 K are provided in Figure S9. The main photophysical parameters are listed in Table 1. It should be noted that, for all complexes, the emission band shapes and wavelengths do not vary by changing the excitation wavelength. As can be seen in Figure 5, both, the mononuclear (**1a-c**) and the Pt-Au (**2a-c**) complexes display similar structured emissions in the solid state, with spectral shape broader at room temperature. The well resolved vibrational progression and the relatively long lifetimes (Table 1) are indicative of excited states of mixed $^3\text{IL}/^3\text{MLCT}$ nature. The slight red shifts observed for the bzq complexes (**1a,b**) in relation to the ppy complex (**1c**) in the precursors is in line with the lower energy gap for the $\pi\pi^*$ orbitals of the more delocalized benzoquinolinyl ligand. A minimal bathochromic shift can be observed for emission bands of the heterobimetallic complexes Pt-Au (**2**), in relation to the Pt precursors (**1**), which is marginal for **2a** and **2b** and more meaningful for **2c** (see Figure S10 for comparison). From 298 to 77 K, the emission bands become intensified and more structured (see Figure S11 for comparison) and a remarkable increase in the luminescence lifetime are observed (Table 1), thus indicating an increase of the ^3IL character for the

emitting excited state. Due to the slight red-shift observed in the emission from **1c** to **2c**, the emission maxima at low temperature for the ppy complex **2c** (489 nm) is very close to that of bzq complexes **2a** and **2b** (494 nm). The photoluminescence quantum yields were measured in the solid state and, therefore, solid state effects cannot be discarded. The benzoquinolinyl-pentafluorophenyl complexes **1a** and **2a** exhibit similar and relatively low quantum yields (ϕ) with values of 3% and 2%, respectively, likely related to a significant quenching associated to extensive intermolecular $\pi\cdots\pi$ interactions. By contrast, complex **1c** with the ppy ligand displays a very high ϕ value (95%), which is drastically reduced to 3.7% by incorporation of the AuCl unit in **2c**. In opposition to **1a** and **1c**, the quantum yield value for **1b** (11 %) is enhanced upon coordination of the AuCl unit in **2b** (29.3%).

As mentioned above, only complex **2a** exhibits a weak emission in CH_2Cl_2 solution at 298 K (Figure S12). However, in the glass state at 77 K, all the complexes are strongly emissive exhibiting well resolved vibronic-structured phosphorescence emission bands (Figure S9). The bands are slightly blue shifted in relation to those observed in the solid state (298 K and 77 K) and are located in a close region (478 – 485 nm) with minimal differences in their maxima. The emission and excitation profiles suggest rather similar electronic transitions.

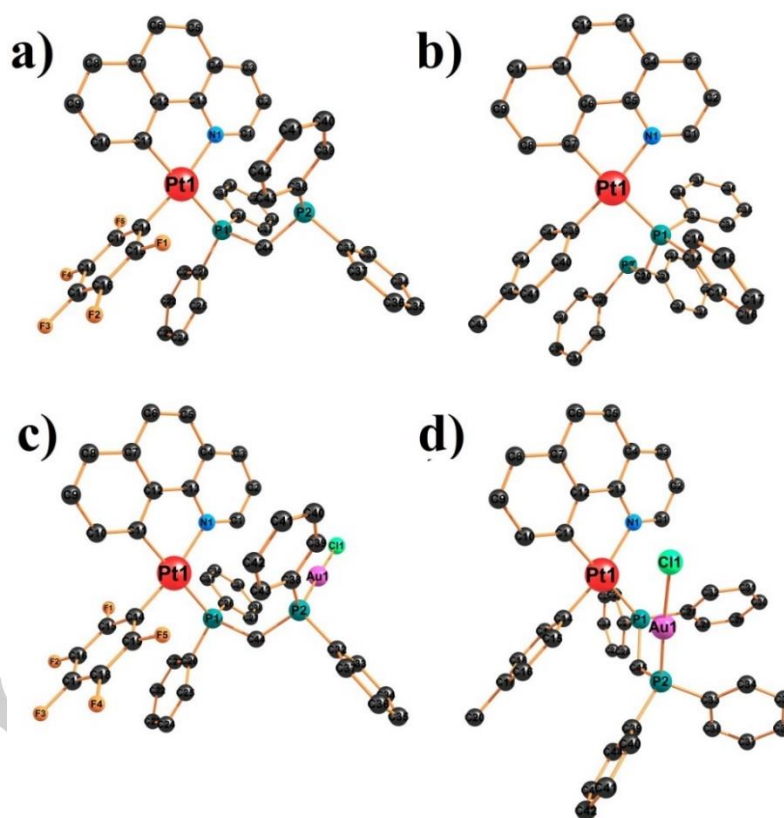


Figure 6. DFT-optimized geometries of a) **1a**, b) **1b**, c) **2a** and d) **2b** in CH_2Cl_2 . Hydrogen atoms were eliminated for clarity.

DFT Calculations

The electronic structures of complexes **1a**, **1b**, **2a** and **2b** were investigated by DFT (density functional theory) calculations. Time-dependent DFT (TD-DFT) calculations were also performed for simulation of the theoretical UV-Vis spectra and to assist in the spectral assignment. For this purpose, the ground states of the

mentioned complexes were optimized in CH_2Cl_2 solvent. The available crystal structures directly or indirectly were used to make input files for the software. The optimized geometries are shown in Figure 6 and corresponding geometrical parameters are collected in Table S3. The calculated structures resemble the crystal structures of **1b**,^[19a] **2a** and **2b**.

FULL PAPER

The energy levels and compositions of selected molecular orbitals for **1a**, **1b**, **2a** and **2b** are listed in Tables S4-S7, respectively. Plots of the highest occupied molecular orbital (HOMO) and lowest unoccupied molecular orbital (LUMO) are

shown in Figure 7, whereas the plots of frontier orbitals including "HOMO to HOMO-10" and "LUMO to LUMO+10", are provided in Figures S13-S16, respectively.

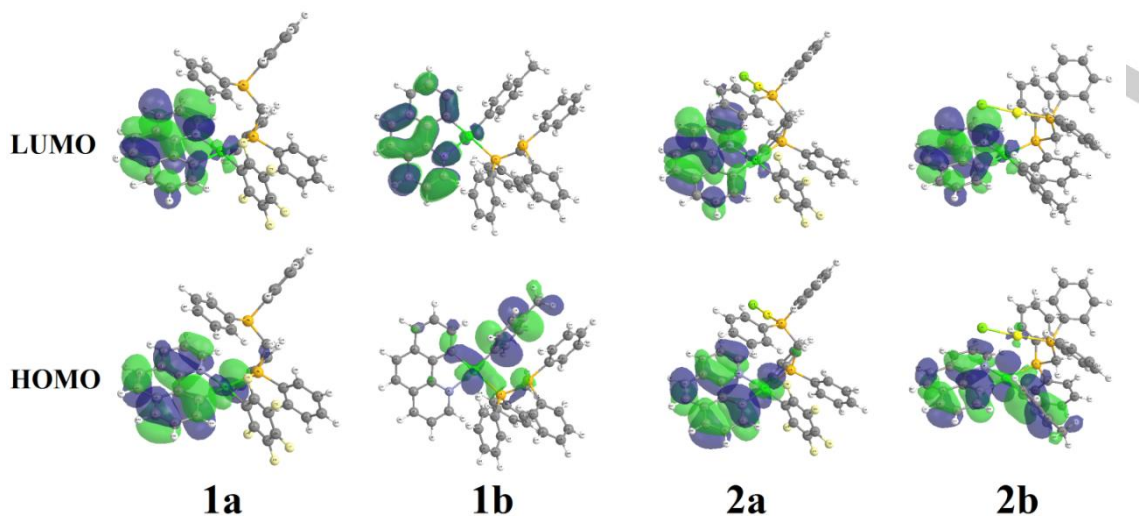


Figure 7. Plots of HOMO and LUMO for **1a**, **1b**, **2a** and **2b**.

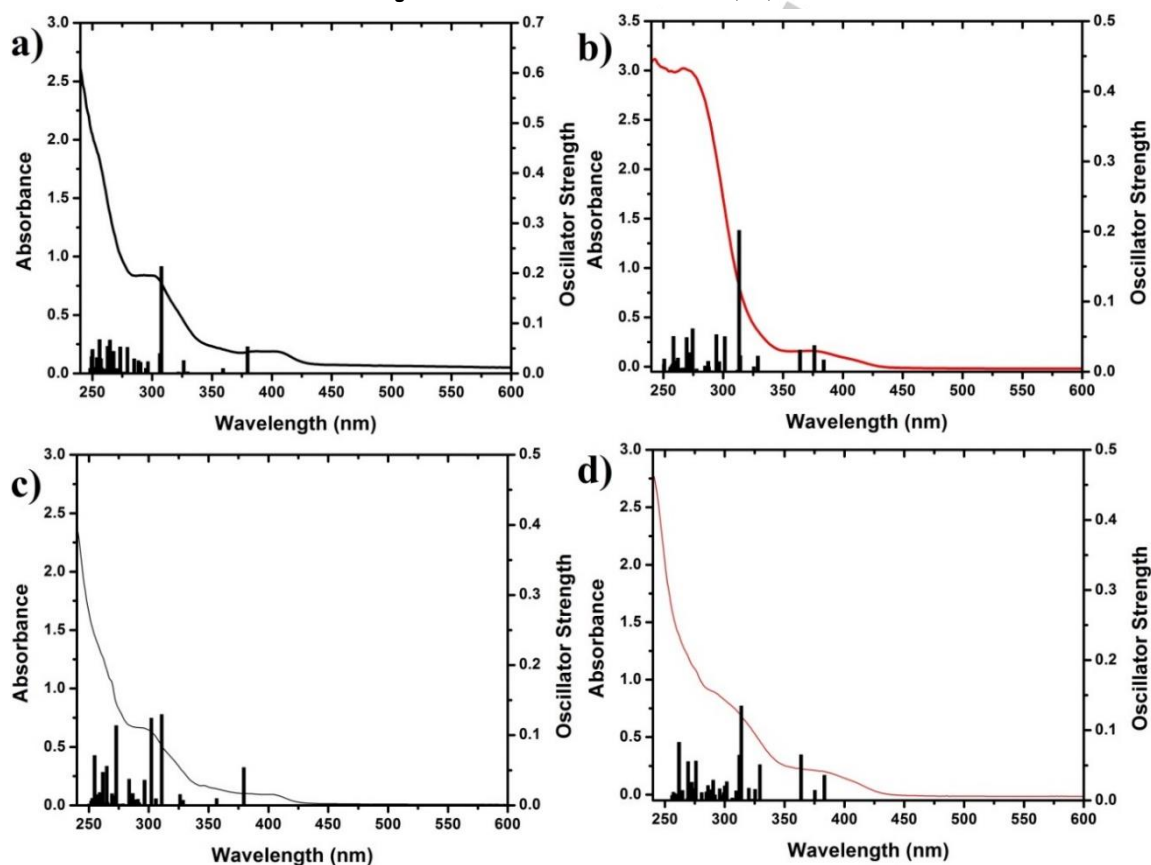


Figure 8. Overlaid experimental (spectra) and theoretical (bars) absorbance for a) **1a**, b) **1b**, c) **2a** and d) **2b**.

For **1a**, the HOMO is located on bzq (71%) and Pt (26%), while in **1b** the HOMO is mostly centered on *p*-MeC₆H₄ ligand (54%) with lower contributions of Pt (27%) and bzq (11%). However, in **1b** the composition of the HOMO-1, which is close in energy (0.086 eV), is similar to the HOMO in **1a** (bzq 66%, Pt 28%). In both complexes, the LUMO and L+1 are almost completely localized on bzq fragment. The contribution of C₆F₅ or

p-MeC₆H₄ is low in most of MOs, while the contribution of dppm becomes important in higher LUMOs or lower HOMOs.

In the heterobimetallic complexes **2a** and **2b**, the composition of the orbital frontiers is rather similar (see Tables S6 and S7) to their precursors **1a** and **1b**, respectively. Thus, in **2a** the HOMO is located on the bzq (72%) and Pt (25%) and the LUMO on the bzq (87%). In **2b**, the HOMO and H-1 are also close

FULL PAPER

in energy (0.044 eV), being contributed from the bzq, Pt and the aryl ligand (*p*-MeC₆H₄ 22% in HOMO and 38% in HOMO-1), whereas the LUMO is centered on bzq fragment (90%). It should be noted that for both complexes the contribution Au-Cl fragment is negligible in most of MOs. However, the contribution of dppm increases from HOMO to HOMO+10 or LUMO to LUMO-10. To further understand the electronic properties of these complexes, TD-DFT calculations were carried out for **1a**, **1b**, **2a** and **2b**. Calculated energies, major contributions, and oscillator strengths of selected spin-allowed electronic transitions together with their corresponding assignments are collected in Tables S8-S11. A comparison of the experimental UV-Vis spectra and the calculated vertical excitations as bars is presented in Figure 8. For the pentafluorophenyl complexes **1a** and **2a**, the first excited state ($S_0 \rightarrow S_1$) is mainly contributed by the HOMO \rightarrow LUMO transition (379 nm) having similar oscillator strength of 0.054, and thus can be described as a mixed ILCT/MLCT (L = bzq, M = Pt) transition.

For **1b** the lowest excited state $S_0 \rightarrow S_1$ is contributed by HOMO and H-1 to LUMO, supporting a mixed ILCT/MLCT/L'LCT (L' = *p*-MeC₆H₄) character. For **2b** the lowest transition $S_0 \rightarrow S_1$ (HOMO \rightarrow LUMO 87%) has also mixed ILCT/MLCT/L'LCT character. In both complexes, the transition is calculated slightly red shifted (383 nm) in relation to **1a** and **2a**, in accordance with the experimental values (exp. 409 nm **1b**, 410 nm **2b** vs 407 nm **1a**, 404 nm **2a**).

As expected, the dppm ligand participates in electronic transitions at higher energies (MLCT and L'LCT, L' = dppm, see Tables S8-11), but the ILCT character still has an outstanding presence. It is worthy to note that Au-Cl fragment in **2a** and **2b** does not participate in any electronic transitions. According to the aryl ligands, in **1a** and **2a**, C₆F₅ has a very negligible contribution in the electronic transitions, while *p*-MeC₆H₄ ligand in **1b** and **2b** exhibit a relatively more effective contribution.

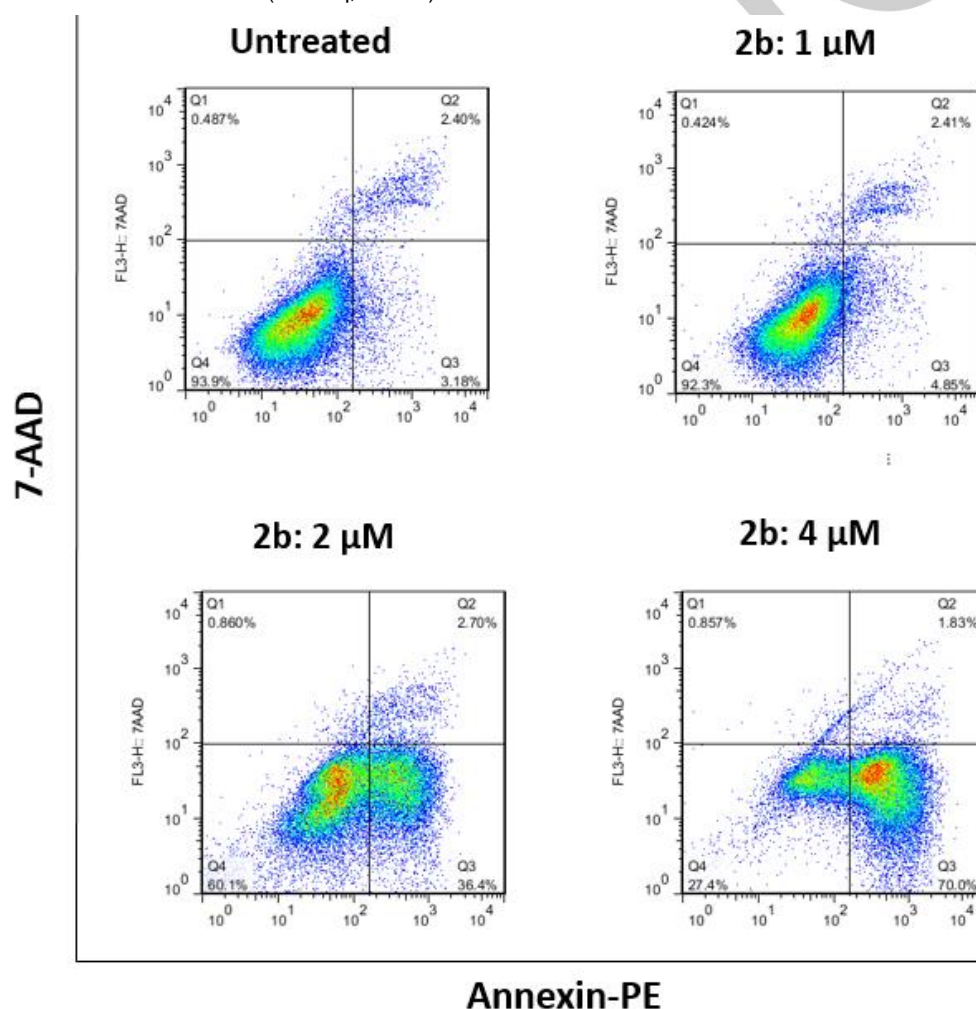


Figure 9. Flow cytometry-based detection of the apoptotic properties of **2b** on MCF-7 cell line. Representative scatter plots show apoptosis of MCF-7 cells after 72 hours of incubation with different concentrations of **2b** (1, 2, and 4 μ M) using the Annexin V-PE/7AAD detection kit. The percentages of apoptotic cells (Q2: late apoptotic and Q3: early apoptotic) were determined in Annexin V+ cells. Q1: necrotic cells, Q2: late apoptotic cells, Q3: early apoptotic cells, and Q4: living cells.

Biological activity studies

The *in vitro* cytotoxic activity of **1a-c** and **2a-c** were evaluated on three human cancer cell lines, MCF-7 (breast cancer), SKOV3 (ovarian cancer), and A549 (non-small cell lung cancer).

As shown in Table 2, **2b**, as the best studied compound, showed a good anti-proliferative activity with an IC₅₀ of 5.47 μ M, 10.73 μ M and 2.27 μ M, compared to that measured for cisplatin, which was 9.63 μ M, 15.66 μ M and 11.34 μ M against the A549, SKOV3 and MCF7 cell lines, respectively. Complex **2c**, also exhibited a higher anti-proliferative activity than cisplatin against

FULL PAPER

A549 and MCF-7 cancer cell lines with IC_{50} of 8.51 μ M, and 3.89 μ M, respectively.

The IC_{50} of Auranofin, as the best-known lead structure of gold(I) complexes, was 6.14 μ M, 6.28 μ M, and 5.17 μ M against the A549, SKOV3, and MCF7 cell lines, respectively. In comparison to Auranofin, **2b** exhibited higher anti-proliferative activity on A549 and, MCF-7, while, **2c** was also showed a higher antitumor activity than Auranofin against MCF-7.

Series of **1a-c**, which have no gold in their structures, as well as $[ClAu(\mu-dppm)AuCl]^{[25]}$ exhibited low potency in inhibiting cell proliferation and significantly lower *in vitro* cytotoxicities against the studied cancer cell lines,^[32] compared to series of **2a-c**. The improvement of the IC_{50} values of the heterometallic complexes suggests a cooperative effect of both metal fragments.

MCF-10A, non-tumorigenic epithelial breast cell line, was used to investigate the selectivity between cancer and the normal cell lines. Results showed good selectivity of the compounds between the tumorigenic and non-tumorigenic cell lines. Interestingly, complexes **2b** and **2c** showed greater specificity for human breast cancer cell with less damage to normal epithelial breast cell.

The structure-activity relationship (SAR) studies on these complexes, revealed that series **2a-c**, which contain dppm bonded to the AuCl, showed considerable antitumor activities compared to the series **1a-c**. The presence of the bzq ligand (in **2b**) had a greater effect on the cytotoxicity than the ppy ligand (in **2c**). On the other hand, the existence of the *p*-MeC₆H₄ as the aromatic group attached to the Pt(II), as it was clear in **2b**, had considerable more cytotoxic effect than the C₆F₅ ligand (in **2a**).

Table 2. *In vitro* cytotoxic activity of the synthesized complexes against three cancerous cell lines (A549, SKOV3 and MCF-7) and non-cancerous cell line (MCF-10A).

| Name | IC_{50} (μ M \pm SD) | | | |
|------------------------|-------------------------------|------------------|------------------|---------|
| | A549 | SKOV3 | MCF-7 | MCF-10A |
| 1a | >100 | >100 | 90.45 \pm 1.06 | >100 |
| 1b | >100 | >100 | >100 | >100 |
| 1c | >100 | >100 | >100 | >100 |
| 2a | 86.32 \pm 2.17 | 95.16 \pm 2.71 | 78.52 \pm 1.38 | >100 |
| 2b | 5.47 \pm 1.32 | 10.73 \pm 1.72 | 2.27 \pm 0.16 | >100 |
| 2c | 8.51 \pm 1.82 | 18.92 \pm 0.28 | 3.89 \pm 0.29 | >100 |
| <i>cisplatin</i> | 9.63 \pm 1.39 | 15.66 \pm 1.34 | 11.34 \pm 1.52 | >100 |
| <i>Auranofin</i> | 6.14 \pm 1.06 | 6.28 \pm 0.67 | 5.17 \pm 0.34 | - |
| $[ClAu(\mu-dppm)AuCl]$ | >100 | >100 | 85.31 \pm 1.27 | - |

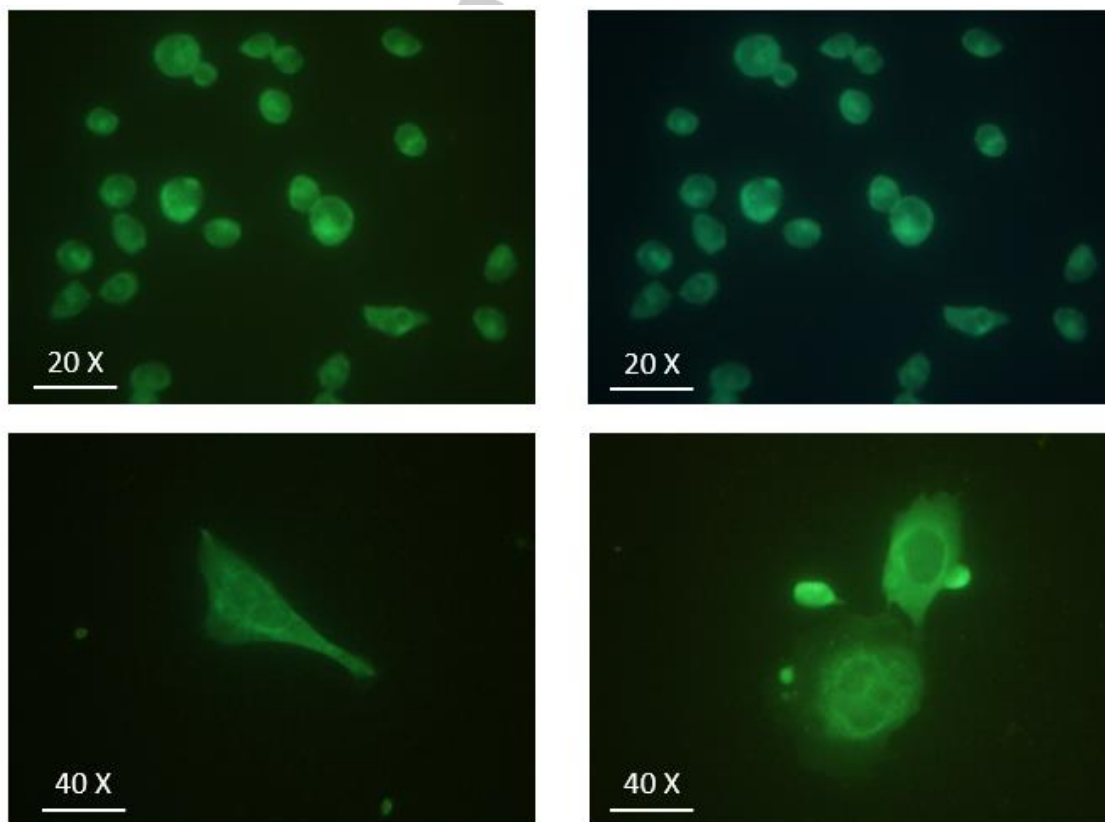


Figure 10. Biological emission and intracellular tracking of compounds **2a** in MCF-7 cells. The cells were treated with 1000 μ M of **2a** for 4 hours and investigated immediately by a fluorescent microscope (See Experimental).

FULL PAPER

Determining apoptotic effect of 2b on MCF-7 cell line

We used BioLegend's PE Annexin V Apoptosis Detection Kit with 7AAD to specifically determine the dose-dependent apoptotic effect of **2b** on cancerous cells. To determine this, complex **2b** with three concentrations (1, 2 and 4 μM) was applied on MCF-7 cells. As illustrated in Figure 9, with the increase in the concentration of **2b** from 1 to 4 μM , the percentage of the cells in early apoptotic phase significantly elevates from 3.18% in untreated cells to 4.85%, 36.40% and 70.00% in the treated cells, respectively. This observation indicated that **2b** compound, is able to effectively induce apoptosis in cancerous cells in a dose dependent manner. It implies that anti-proliferative/cytotoxic effect observed for **2b** in cytotoxic assay, could be mediated through inducing apoptosis in cancer cells.

Fluorescence microscopy cellular localization on 2a

Due to the emissive properties of **2a** in solution, its intracellular localization was assessed by fluorescence microscopy imaging (see experimental for details). As illustrated in Figure 10, the MCF-7 cells treated with 1000 μM of **2a** for 4 hours show green-blue light emission. As could be observed, **2a** were efficiently penetrated into the cells, mostly localized in the nucleus with less dispersion in the cytoplasm of MCF-7 cells.^[12b]

Conclusions

To be concluded, a series of closely related cyclometalated Pt(II) with monodentate dpmm (**1a-c**) and their corresponding cyclometalated Pt(II)-Au(I) complexes (**2a-c**) were successfully prepared and characterized. In the heterobimetallic complexes, dpmm ligand was situated as an unsymmetrical bridge between the Pt(II) and Au(I) centers. The crystal structures of Pt(II)-Au(I) complexes showed no Pt(II)-Au(I) bonding interaction in these heterobimetallic complexes. The absence of these Pt(II)-Au(I) bonds causes that the electronic structures do not remarkably change in relation to those of Pt(II) parent complexes, as evidenced by spectroscopy (absorption and emission) and supported by DFT and TDDFT calculations on selected **1a**, **1b**, **2a** and **2b** complexes. These complexes are only emissive in rigid media exhibiting typical structured bands with well resolved vibrational progression and relatively long lifetime's characteristic of excited states of mixed $^3\text{IL}^3\text{MLCT}$ nature with remarkable strong intraligand (cyclometalated) character. The heterometallic Pt-Au complexes show an improvement of the *in vitro* cytotoxic activity against A549 (lung), SKOV3 (ovarian) and MCF-7 (breast) cancer cell lines in comparison to complexes **1** and [ClAu(μ -dpmm)AuCl], suggesting a cooperative effect of the metal fragments. Complex **2b** exhibited high potency in inhibiting cell proliferation compared to cisplatin and Auranofin, and can effectively induce apoptosis in MCF-7 cells in a dose dependent manner. Also, the effects of complexes **2b** and **2c** on the proliferation of the non-tumorigenic epithelial breast (MCF-10A) revealed good selectivity among the tumorigenic and non-tumorigenic cell lines. Fluorescence microscopy revealed effective localization of **2a** into MCF-7 human cells.

Experimental Section**General procedures and materials**

The reactions were fully performed in common solvents without any further purification. All NMR spectra [^1H (400 MHz), $^{31}\text{P}\{^1\text{H}\}$ (161.9 MHz),

$^{19}\text{F}\{^1\text{H}\}$ (376.5 MHz)] were recorded on a Bruker Avance DPX 400 MHz instrument. The ^1H NMR spectra were referenced to the residual peak of the solvents, i.e. CDCl_3 and CD_3COCD_3 , while the $^{31}\text{P}\{^1\text{H}\}$ NMR and $^{19}\text{F}\{^1\text{H}\}$ NMR spectra were referenced to the external 85% H_3PO_4 and CFCl_3 , respectively. The chemical shifts (δ) being reported as ppm and coupling constants (J) expressed in Hz. Elemental analyses were carried out with a Carlo Erba EA1110 CHNS/O microanalyzer. Electrospray ion mass spectra (ESI-MS) were recorded using a HP-5989B spectrometer using methanol-water as the mobile phase. The UV-Vis absorption spectra were carried out in a Hewlett-Packard 8453 spectrophotometer. Diffuse reflectance UV-Vis (DRUV) data of pressed powder were recorded on a Shimadzu (UV-3600 spectrophotometer with a Harrick Praying Mantis accessory) and recalculated following the Kubelka-Munk function. Excitation and emission spectra were obtained on a Jobin-Yvon Horiba Fluorolog 3-11 Tau-3 spectrofluorimeter. The lifetime measurements were performed in a Jobin Yvon Horiba Fluorolog operating in the phosphorimeter mode (with an F1-1029 lifetime emission PMT assembly, using a 450W Xe lamp) or with a Datastation HUB-B with a nanoLED controller and software DAS6. The nanoLEDs employed for lifetime measurements were of wavelength 450 nm with pulse lengths of 0.8-1.4 ns. The lifetime data were fitted using the Jobin-Yvon software package. Quantum yields in solid were measured using an F-3018 Integrating Sphere mounted on a Fluorolog 3-11 Tau-3 spectrofluorimeter. The complexes [Pt(bzq)(C_6F_5)(dmsO)], **A**,^[33] [Pt(bzq)(p -MeC $_6$ H $_4$)(dmsO)], **B**,^[34] [Pt(ppy)(p -MeC $_6$ H $_4$)(dmsO)], **C**,^[34] [Pt(bzq)(p -MeC $_6$ H $_4$)(κ^1 -dpmm)], **1b**,^[19a] [Pt(ppy)(p -MeC $_6$ H $_4$)(κ^1 -dpmm)], **1c**,^[19a] [AuCl(SMe $_2$)]^[25] and [ClAu(μ -dpmm)AuCl]^[25] were prepared as reported in the literature. The chemical shift assignments are based on the NMR labeling for the ligands as are shown in Scheme 1.

Synthesis of the complexes

[Pt(bzq)(C_6F_5)(κ^1 -dpmm)], **1a**. To a yellow suspension of **A** (0.150 gr, 0.243 mmol) in acetone (25 mL), dpmm (0.093 gr, 0.2425 mmol) was added. After 30 min of stirring, the solution obtained was evaporated to dryness and treated with hexane (5 mL) and cold isopropanol (2 mL) to afford **1a** as a yellow solid. Yield = 58%. Anal. Calcd. for $\text{C}_{44}\text{H}_{30}\text{F}_5\text{NP}_2\text{Pt}$ (924.73): C, 57.15; H, 3.27; N, 1.51%. Found: C, 56.89; H, 3.53; N, 1.78%. ESI (+): m/z (%) 757 [M-C $_6\text{F}_5$]⁺ (100). NMR data in CD_3COCD_3 : δ (^1H): 3.65 (d, 1H, $J = 9$, $^3J_{\text{Pt-H}} = 26$, CH $_2$ P $_2$), 6.92-6.88 (m, 6H), 6.96 (t, 1H, $^3J_{\text{H-H}} \approx ^4J_{\text{P-H}} = 6$, H 9 , bzq), 7.14 (dd, 1H, $J = 8$, $J = 5$, H 3 , bzq), 7.44-7.39 (m, 3H), 7.36-7.33 (m, 4H), 7.66 (t, 2H, $J = 8$), 7.53 (m, 4H), 7.88 (m, 5H), 8.25 (t, 4H, $J = 5$, $^3J_{\text{Pt-H}} = 24$, H 2 , bzq), 8.39 (d, $J = 8$, H 4 , bzq); δ ($^{31}\text{P}\{^1\text{H}\}$): 12.62 (d, $^2J_{\text{PP}} = 13$, $^1J_{\text{P-Pt}} = 1963$), -25.3 (dm, $^2J_{\text{PP}} = 13$ Hz, $^3J_{\text{P-Pt}}$ not resolved); δ ($^{19}\text{F}\{^1\text{H}\}$): -115.7 (dm, $J_{\text{Pt-F}} = 496$, 2o-F, C $_6\text{F}_5$), from -166.5 to -166.9 (m, 1p-F, 2m-F, C $_6\text{F}_5$).

[Pt(bzq)(C_6F_5)(κ^1 -dpmmO)], **1aO**. NMR data in CDCl_3 : δ (^1H): 3.34 (dd, $J = 12$, $J = 8$, $^3J_{\text{Pt-H}} = 33$, CH $_2$ P $_2$), 6.99-6.93 (m, 2H, H 3,9 , bzq), 7.14-7.12 (m, 6H), 7.27-7.23 (m, 4H), 7.36-7.32 (m, 2H), 7.44 (td, 1H, $J = 7$, $^5J_{\text{H-P}} = 2$, H 8 , bzq), 7.47 (d, $J = 8$, 1H), 7.61-7.54 (m, 5H), 7.75 (d, $J = 8$, 1H), 8.00-7.95 (m, 4H), 8.12 (dd, 1H, $J = 8$, $^4J_{\text{H-H}} = 1$, H 4 , bzq), 8.20 (d, 1H, $J = 5$, $^3J_{\text{Pt-H}} = 23$, H 2 , bzq); δ ($^{31}\text{P}\{^1\text{H}\}$): 25.30 (d, $^2J_{\text{PP}} = 13$, $^3J_{\text{P-Pt}} = 46$), 12.75 (d, $^2J_{\text{PP}} = 13$, $^1J_{\text{P-Pt}} = 1950$); δ ($^{19}\text{F}\{^1\text{H}\}$): -116.2 (dm, $J_{\text{Pt-F}} = 490$, 2o-F, C $_6\text{F}_5$), -163.3 (t, 1p-F, C $_6\text{F}_5$), -163.8 (m, 2m-F, C $_6\text{F}_5$).

[Pt(bzq)(C_6F_5)(μ -dpmm)AuCl], **2a**. [AuCl(SMe $_2$)] (0.02 gr, 0.093 mmol) was added to a solution of **1a** (0.086 gr, 0.093 mmol) in CH_2Cl_2 (20 mL) at -50 $^\circ\text{C}$. After 10 min of stirring, the yellow solution was evaporated until 5 mL and a yellow solid was precipitated with hexane (~10 mL) to obtain **2a** as a yellow solid. Yield = 44 %. Anal. Calcd. for $\text{C}_{44}\text{H}_{30}\text{F}_5\text{NP}_2\text{ClPtAu}$ (1157.15): C, 45.67; H, 2.61; N, 1.21%. Found: C, 45.28; H, 2.87; N, 1.49%. ESI (+): m/z (%) 1180 [M + Na]⁺ (12). NMR data in CDCl_3 : δ (^1H): 3.63 (dd, $J = 11$, $J = 7$, $^3J_{\text{Pt-H}} = 34$, CH $_2$ P $_2$), 6.88 (t, 1H, $^3J_{\text{H-H}} \approx ^4J_{\text{P-H}} = 6$, H 9 , bzq), 7.12-7.04 (m, 6H), 7.24 (d, 1H, $J = 5$, H 3 , bzq), 7.37-7.33 (m, 4H), 7.40 (td, 1H, $J = 7$, $^5J_{\text{H-P}} = 2$, H 8 , bzq), 7.48-7.44 (m, 3H), 7.64-7.57 (m, 5H), 7.75-7.71 (m, 5H), 8.17 (dd, 1H, $J = 8$, $^4J_{\text{H-H}} = 1$, H 4 , bzq), 8.74 (d, 1H, $J = 5$, $^3J_{\text{Pt-H}} = 25$, H 2 , bzq); δ ($^{31}\text{P}\{^1\text{H}\}$): 19.07 (d, $^2J_{\text{PP}} = 4$, $^3J_{\text{P-Pt}} = 23$), 12.2 (s br, $^2J_{\text{PP}}$ not resolved, $^1J_{\text{P-Pt}} = 1890$); δ ($^{19}\text{F}\{^1\text{H}\}$): -116.6 (dm, $J_{\text{Pt-F}} = 475$, 2o-F, C $_6\text{F}_5$), -163.2 (t, 1p-F, C $_6\text{F}_5$), -163.8 (m, 2m-F, C $_6\text{F}_5$).

[Pt(bzq)(p -MeC $_6$ H $_4$)(μ -dpmm)Au(Cl)], **2b**. To a solution of **1b** (0.04 gr, 0.05 mmol) in CH_2Cl_2 (15 mL), [AuCl(SMe $_2$)] (0.014 gr, 0.05 mmol) was added. The mixture was stirred at room temperature for 3 h under an Ar atmosphere. After concentration of the solvent, the residue was washed with diethyl ether. The precipitate was filtered and washed with diethyl ether to give the product as a yellow solid. Yield: 90%. Anal. Calcd. For $\text{C}_{45}\text{H}_{37}\text{ClINP}_2\text{PtAu}$ (1081.23): C, 49.99; H, 3.45; N, 1.30%; Found: C, 50.37; H, 3.54; N, 1.21%. ESI (+): m/z (%) 1082 [M + H]⁺ (100). NMR data in CDCl_3 : δ (^1H): 2.22 (s, 3H, Me, p -MeC $_6$ H $_4$), 3.06 (dd, $^2J_{\text{PH}} = 8.1$, $^3J_{\text{PH}} = 37.5$, 2H, CH $_2$ P $_2$), 6.74 (d, $^3J_{\text{HH}} = 7.5$, 2H), 6.95 (dd, $^3J_{\text{HH}} = 7.1$, $^3J_{\text{HH}} = 6.5$,

FULL PAPER

1H), 7.17-7.45 (m, 15H), 7.50 (m, 3H, H^o and H⁹, bzzq), 7.55-7.61 (m, 2H), 7.62-7.69 (m, 1H), 7.76-7.89 (m, 2H), 7.94-8.03 (m, 4H), 8.16 (d, ³J_{HH} = 7.1, ³J_{PH} = 59.1, 2H); δ (³¹P) 18.36 (d, ¹J_{PP} = 2032.2, ²J_{PP} = 14.5, 1P), 19.67 (d, ³J_{PP} = 84.3, ²J_{PP} = 14.6, 1P).

[Pt(ppy)(p-MeC₆H₄)(μ-dppm)Au(Cl)]₂, 2c. To a solution of **1c** (0.072 gr, 0.08 mmol), in CH₂Cl₂ (15 mL), [AuCl(SMe₂)] (0.026 gr, 0.08 mmol) was added. The solution was stirred under an Ar atmosphere for 3 h at room temperature, then concentrated to a small volume (2 mL) and treated with diethyl ether (5 mL). The formed precipitate was filtered off, washed with diethyl ether to give the product as a green-yellow solid. The precipitate was dried in vacuum. Yield: 92%. Anal. Calcd. For C₄₃H₃₇ClN₂PtAu (1057.21): C, 48.85; H, 3.53; N, 1.32%; Found: C, 48.93; H, 3.51; N, 1.37%. ESI (+): *m/z* (%) 1058 [M + H]⁺ (100). NMR data in CDCl₃: δ (¹H) 2.17 (s, 3H, Me, *p*-MeC₆H₄), 2.94 (dd, ²J_{PH} = 8.2, ³J_{PH} = 39.6, 2H, CH₂P₂), 6.56 (t, ³J_{HH} = 6.5, 1H), 6.65 (d, ³J_{HH} = 7.4, 2H), 7.03-7.40 (m, 17H), 7.45 (m, 3H, H^o and H³, ppy), 7.62-7.83 (m, 4H), 7.88-8.00 (m, 5H); δ (³¹P) 19.00 (d, ¹J_{PP} = 1960.0, ²J_{PP} = 17.1, 1P), 19.75 (d, ³J_{PP} = 83.7, ²J_{PP} = 17.1, 1P).

Biological assay**Cell lines and cell culture**

Human cancer cell lines, MCF-7 (breast cancer), SKOV3 (ovarian cancer), and A549 (non-small cell lung cancer) were purchased from National Cell Bank of Iran (NCBI, Pasteur Institute, Tehran, Iran). The cells were grown in complete culture media containing RPMI 1640 (Biosera, France), 10% fetal bovine serum (FBS; Gibco, USA) and 1% penicillin-streptomycin (Biosera, France) and kept at 37 °C in a humidified CO₂ incubator. MCF10A cells (human breast epithelial cell line) were cultured in DMEM/Ham's F-12 (GIBCO-Invitrogen, Carlsbad, CA) supplemented with 100 ng/ml cholera toxin, 20 ng/ml epidermal growth factor (EGF), 0.01 mg/ml insulin, 500 ng/ml hydrocortisone, and 5% chelex-treated horse serum.

Cytotoxic activities of the synthesized compounds were investigated using a standard 3-(4,5-dimethylthiazol-yl)-2,5-diphenyl-tetrazolium bromide (MTT) assay, as previously described.^[35] To do this, the cells with a density of 0.8 × 10⁴ cells per well were seeded in 96-well microplates and kept for 24h to recover. The cells were then treated with the synthesized compounds in different concentrations from 1 to 100 μM in a triplicate manner and incubated for more 72 hours at 37 °C in humidified CO₂ incubator. Following incubation, the media were completely discarded and replaced with 150 μl of RPMI 1640 containing 0.5 mg/mL MTT solution and incubated at room temperature for 3h. To dissolve the formazan crystals, the media containing MTT was discarded again and 150 μl of DMSO was added to each well and incubated for more 30 min at 37 °C in the dark. The absorbance of individual well was then read at 490 nm with an ELISA reader. The 50% inhibitory concentration of each compound, representing IC₅₀, was calculated using CurveExpert 1.4. Data are presented as mean ± SD.

Apoptosis assay

BioLegend's PE Annexin V Apoptosis Detection Kit with 7AAD (Biolegend, USA) was used to assess the apoptotic effect of **2b** as previously described.^[35] Briefly, 0.5 × 10⁵ cells per 1 ml of complete culture medium were seeded in a 24-well culture plate, treated with **2b** compound in different concentrations (1, 2 and 4 μM) for 72 h. An untreated sample was also included as a negative control. Treated and untreated cells were then harvested and washed twice with cold BioLegend's Cell Staining Buffer, transferred to the polystyrene round-bottom tubes (BD Bioscience, USA) and stained with 2 μl of PE-conjugated Annexin V and 2 μl of 7-AAD solution for 15 min at room temperature in the dark. 300 μl of Binding Buffer was added to each tube and analyzed immediately by four-color FACSCalibur flow cytometer (BD Bioscience, USA) with proper setting. The data were analyzed by FlowJo software packages.

Biological emission and intracellular localization of 2a

Due to the fluorescence emission properties of our compounds, the ability to track **2a** in the biological relevant media and tumor cells were checked using fluorescent microscopy imaging. To assess, as previously described,^[12b] the MCF-7 cells were cultured over coverslips in a 6-well plate in complete culture media for 24 h. The cells were then incubated with 1000 μM of **2a** at 37 °C for 4 h. The cells were then washed twice in 1× Phosphate Buffer Saline (PBS, pH=7.2) and fixed with cold absolute methanol for 15 min (Merck, Germany). Following drying in room temperature, the cell covered by glycerol, mounted on glass slides and were immediately observed under a fluorescence microscope (BX61,

Olympus, Japan). The images were taken at 20x and 40x magnification and analyzed by the Olympus micro imaging software cellSens (Olympus, Japan). The emission of compound could be detected at two channels (Excitation=365/10, Emission=420LP and Excitation=535/30, Emission=580LP).

CCDC-1860146 (**1aO**), CCDC-1860147 (**2a**) and CCDC-1860148 (**2b**) contain the supplementary crystallographic data for this paper. This data can be obtained free of charge from The Cambridge Crystallographic Data Centre via www.ccdc.cam.ac.uk/data_request/cif.

Supporting Information (see footnote on the first page of this article): NMR spectra, ESI-MS spectra, crystallographic and computational details.

Acknowledgements

This work was supported by the Institute for Advanced Studies in Basic Sciences (IASBS) Research Council (G2018IASBS32629) and the Spanish MINECO (Project CTQ2016-78463-P). N.G. is grateful for a UR grant. M. F. is grateful to the Medicinal Chemistry, school of pharmacy, Ahvaz Jundishapur University of Medical Sciences (GP96075) and the Iran National Science Foundation (Grant no 96007334).

Keywords: Heterobimetallic complexes • Cycloplatinated complexes • Photophysical properties • Cytotoxic study • Bis(diphenylphosphino)methane ligand.

- [1] a) J. R. Berenguer, E. Lalinde, M. T. Moreno, *Coord. Chem. Rev.* **2018**, 366, 69-90; b) M. Yoshida, M. Kato, *Coord. Chem. Rev.* **2018**, 355, 101-115.
- [2] a) A. Zanardi, R. Corberán, J. A. Mata, E. Peris, *Organometallics* **2008**, 27, 3570-3576; b) A. Zanardi, J. A. Mata, E. Peris, *J. Am. Chem. Soc.* **2009**, 131, 14531-14537; c) S. Sabater, J. A. Mata, E. Peris, *Organometallics* **2012**, 31, 6450-6456.
- [3] a) R. D. Adams, B. Captain, *J. Organomet. Chem.* **2004**, 689, 4521-4529; b) R. D. Adams, *J. Organomet. Chem.* **2000**, 600, 1-6; c) R. D. Adams, T. S. Barnard, *Organometallics* **1998**, 17, 2885-2890.
- [4] a) M. Wenzel, A. De Almeida, E. Bigaeva, P. Kavanagh, M. Picquet, P. Le Gendre, E. Bodio, A. Casini, *Inorg. Chem.* **2016**, 55, 2544-2557; b) L. Ma, X. Lin, C. Li, Z. Xu, C.-Y. Chan, M.-K. Tse, P. Shi, G. Zhu, *Inorg. Chem.* **2018**, 57, 2917-2924; c) M. Wenzel, E. Bigaeva, P. Richard, P. Le Gendre, M. Picquet, A. Casini, E. Bodio, *J. Inorg. Biochem.* **2014**, 141, 10-16; d) J. F. González-Pantoja, M. Stern, A. A. Jarzecki, E. Royo, E. Robles-Escajeda, A. Varela-Ramírez, R. J. Aguilera, M. Contel, *Inorg. Chem.* **2011**, 50, 11099-11110; e) B. Bertrand, A. Citta, I. L. Franken, M. Picquet, A. Folda, V. Scalcon, M. P. Rigobello, P. Le Gendre, A. Casini, E. Bodio, *J. Biol. Inorg. Chem.* **2015**, 20, 1005-1020; f) F. Pelletier, V. Comte, A. Massard, M. Wenzel, S. Toulou, P. Richard, M. Picquet, P. Le Gendre, O. Zava, F. Edefe, *J. Med. Chem.* **2010**, 53, 6923-6933; g) L. Massai, J. Fernández-Gallardo, A. Guerri, A. Arcangeli, S. Pillozzi, M. Contel, L. Messori, *Dalton Trans.* **2015**, 44, 11067-11076.
- [5] a) N. A. Vyas, S. B. Singh, A. S. Kumbhar, D. S. Ranade, G. R. Walke, P. P. Kulkarni, V. Jani, U. B. Sonavane, R. R. Joshi, S. Rapole, *Inorg. Chem.* **2018**, 57, 7524-7535; b) Y. Zaidi, F. Arjmand, N. Zaidi, J. A. Usmani, H. Zubair, K. Akhtar, M. Hossain, G. G. H. A. Shadab, *Metallomics* **2014**, 6, 1469-1479; c) L. Boselli, M. Carraz, S. Mazères, L. Paloque, G. González, F. Benoit-Vical, A. Valentin, C. Hemmert, H. Gornitzka, *Organometallics* **2015**, 34, 1046-1055; d) A. Luengo, V. Fernández-Moreira, I. Marzo, M. C. Gimeno, *Inorg. Chem.* **2017**, 56, 15159-15170.
- [6] a) W. S. McDonald, P. G. Pringle, B. L. Shaw, *J. Chem. Soc., Chem. Commun.* **1982**, 861-864; b) P. G. Pringle, B. L. Shaw, *J. Chem. Soc., Chem. Commun.* **1982**, 1313-1314; c) H.-K. Yip, C.-M. Che, S.-M. Peng, *J. Chem. Soc., Chem. Commun.* **1991**, 1626-1628; d) P. G. Pringle, B. L. Shaw, *J. Chem. Soc., Dalton Trans.* **1984**, 849-853; e) G. R. Cooper, A. T. Hutton, C. R. Langrick, D. M. McEwan, P. G. Pringle, B. L. Shaw, *J.*

FULL PAPER

- Chem. Soc., Dalton Trans.* **1984**, 855-862; f) C. R. Langrick, P. G. Pringle, B. L. Shaw, *J. Chem. Soc., Dalton Trans.* **1984**, 1233-1238; g) H.-K. Yip, H.-M. Lin, K.-K. Cheung, C.-M. Che, Y. Wang, *Inorg. Chem.* **1994**, *33*, 1644-1651; h) H.-K. Yip, H.-M. Lin, Y. Wang, C.-M. Che, *J. Chem. Soc., Dalton Trans.* **1993**; i) A. L. Balch, V. J. Catalano, M. M. Olmstead, *Inorg. Chem.* **1990**, *29*, 585-586; j) T. R. Cook, A. J. Esswein, D. G. Nocera, *J. Am. Chem. Soc.* **2007**, *129*, 10094-10095; k) G. Douglas, L. Manojlovic-Muir, K. W. Muir, M. C. Jennings, B. R. Lloyd, M. Rashidi, G. Schoettel, R. J. Puddephatt, *Organometallics* **1991**, *10*, 3927-3933; l) G.-Q. Yin, Q.-H. Wei, L.-Y. Zhang, Z.-N. Chen, *Organometallics* **2006**, *25*, 580-587; m) C. Xu, G. K. Anderson, L. Brammer, J. Braddock-Wilking, N. P. Rath, *Organometallics* **1996**, *15*, 3972-3979; n) L.-Y. Zhang, L.-J. Xu, J.-Y. Wang, X.-C. Zeng, Z.-N. Chen, *Dalton Trans.* **2017**, *46*, 865-874.
- [7] a) W. Lu, B.-X. Mi, M. C. Chan, Z. Hui, C.-M. Che, N. Zhu, S.-T. Lee, *J. Am. Chem. Soc.* **2004**, *126*, 4958-4971; b) E. Rossi, L. Murphy, P. L. Brothwood, A. Colombo, C. Dragonetti, D. Roberto, R. Ugo, M. Cocchi, J. G. Williams, *J. Mater. Chem.* **2011**, *21*, 15501-15510; c) A. Y.-Y. Tam, D. P.-K. Tsang, M.-Y. Chan, N. Zhu, V. W.-W. Yam, *Chem. Commun.* **2011**, *47*, 3383-3385; d) E. S.-H. Lam, D. P.-K. Tsang, W. H. Lam, A. Y.-Y. Tam, M.-Y. Chan, W.-T. Wong, V. W.-W. Yam, *Chem. Eur. J.* **2013**, *19*, 6385-6397; e) A. J. Huckaba, B. Cao, T. K. Hollis, H. U. Valle, J. T. Kelly, N. I. Hammer, A. G. Oliver, C. E. Webster, *Dalton Trans.* **2013**, *42*, 8820-8826.
- [8] B. Pashaei, H. Shahroosvand, M. Graetzel, M. K. Nazeeruddin, *Chem. Rev.* **2016**, *116*, 9485-9564.
- [9] a) V. W. W. Yam, R. P. L. Tang, K. M. C. Wong, X. X. Lu, K. K. Cheung, N. Zhu, *Chem. Eur. J.* **2002**, *8*, 4066-4076; b) P.-H. Lanoë, H. Le Bozec, J. G. Williams, J.-L. Fillaut, V. Guerschais, *Dalton Trans.* **2010**, *39*, 707-710; c) P. K. Siu, S. W. Lai, W. Lu, N. Zhu, C. M. Che, *Eur. J. Inorg. Chem.* **2003**, *2003*, 2749-2752.
- [10] a) A. F. Rausch, H. H. Homeier, H. Yersin, in *Photophysics of Organometallics* (Ed.: A. J. Lees), Springer, **2010**, pp. 193-235; b) L. Murphy, J. G. Williams, in *Molecular Organometallic Materials for Optics*, Springer, **2010**, pp. 75-111; c) H. Yersin, *Highly efficient OLEDs with phosphorescent materials*, John Wiley & Sons, **2008**.
- [11] N. M. Shavaleev, H. Adams, J. Best, R. Edge, S. Navaratnam, J. A. Weinstein, *Inorg. Chem.* **2006**, *45*, 9410-9415.
- [12] a) J. Liu, C.-H. Leung, A. L.-F. Chow, R. W.-Y. Sun, S.-C. Yan, C.-M. Che, *Chem. Commun.* **2011**, *47*, 719-721; b) M. Fereidoonzehad, B. Kaboudin, T. Mirzaee, R. Babadi Aghakhanpour, M. Golbon Haghghi, Z. Faghhih, Z. Faghhih, Z. Ahmadipour, B. Notash, H. R. Shahsavari, *Organometallics* **2017**, *36*, 1707-1717.
- [13] a) J. A. Gareth Williams, S. Develay, D. L. Rochester, L. Murphy, *Coord. Chem. Rev.* **2008**, *252*, 2596-2611; b) H. Yersin, A. F. Rausch, R. Czerwieńiec, T. Hofbeck, T. Fischer, *Coord. Chem. Rev.* **2011**, *255*, 2622-2652; c) H. R. Shahsavari, R. Babadi Aghakhanpour, M. Nikravesh, J. Ozdemir, M. Golbon Haghghi, B. Notash, M. H. Beyzavi, *Organometallics* **2018**, *37*, 2890-2900.
- [14] a) T. Yamaguchi, F. Yamazaki, T. Ito, *J. Am. Chem. Soc.* **2001**, *123*, 743-744; b) D. E. Janzen, L. F. Mehne, D. G. VanDerveer, G. J. Grant, *Inorg. Chem.* **2005**, *44*, 8182-8184; c) J. Forniés, S. Ibáñez, A. Martín, M. Sanz, J. R. Berenguer, E. Lalinde, J. Torroba, *Organometallics* **2006**, *25*, 4331-4340; d) S. Jamali, Z. Mazloomi, S. M. Nabavizadeh, D. Milić, R. Kia, M. Rashidi, *Inorg. Chem.* **2010**, *49*, 2721-2726; e) S. Fuentès, A. J. Chueca, A. Martín, V. Sicilia, *Cryst. Growth Des.* **2017**, *17*, 4336-4346; f) S. Fuentès, C. H. Woodall, P. R. Raithby, V. Sicilia, *Organometallics* **2012**, *31*, 4228-4240; g) J. R. Berenguer, E. Lalinde, A. Martín, M. T. Moreno, S. Sánchez, H. R. Shahsavari, *Inorg. Chem.* **2016**, *55*, 7866-7878; h) M. J. Karimi, S. Jamali, *J. Organomet. Chem.* **2015**, *786*, 14-20; i) S. Horiuchi, S. Moon, E. Sakuda, A. Ito, Y. Arikawa, K. Umakoshi, *Dalton Trans.* **2018**, *47*, 7113-7117; j) J. Moussa, A. Loch, L.-M. Chamoreau, A. Degli Esposti, E. Bandini, A. Barbieri, H. Amouri, *Inorg. Chem.* **2017**, *56*, 2050-2059.
- [15] a) H. Molaee, S. M. Nabavizadeh, M. Jamshidi, M. Vilsmeier, A. Pfitzner, M. Samandar Sangari, *Dalton Trans.* **2017**, *46*, 16077-16088; b) R. Muñoz-Rodríguez, E. Buñuel, N. Fuentes, J. G. Williams, D. J. Cárdenas, *Dalton Trans.* **2015**, *44*, 8394-8405; c) R. Packheiser, P. Ecorchard, B. Walfort, H. Lang, *J. Organomet. Chem.* **2008**, *693*, 933-946; d) C. H. Shin, J. O. Huh, S. J. Baek, S. K. Kim, M. H. Lee, Y. Do, *Eur. J. Inorg. Chem.* **2010**, *2010*, 3642-3651; e) J. Forniés, S. Fuentès, A. Martín, V. Sicilia, E. Lalinde, M. T. Moreno, *Chem. Eur. J.* **2006**, *12*, 8253-8266; f) S. Back, R. A. Gossage, H. Lang, G. van Koten, *Eur. J. Inorg. Chem.* **2000**, *2000*, 1457-1464; g) S. Back, R. A. Gossage, M. Lutz, I. del Río, A. L. Spek, H. Lang, G. van Koten, *Organometallics* **2000**, *19*, 3296-3304; h) S. Yamaguchi, H. Shinokubo, A. Osuka, *Inorg. Chem.* **2009**, *48*, 795-797; i) H. Sesolis, C. K.-M. Chan, G. Gontard, H. L.-K. Fu, V. W.-W. Yam, H. Amouri, *Organometallics* **2017**, *36*, 4794-4801; j) G. Ferraro, G. Petruk, L. Maiore, F. Pane, A. Amoresano, M. A. Cinellu, D. M. Monti, A. Merlino, *Int. J. Biol. Macromol.* **2018**, *115*, 1116-1121.
- [16] a) N. Cutillas, G. S. Yellol, C. de Haro, C. Vicente, V. Rodríguez, J. Ruiz, *Coord. Chem. Rev.* **2013**, *257*, 2784-2797; b) I. Omae, *Coord. Chem. Rev.* **2014**, *280*, 84-95; c) A. Zamora, S. A. Pérez, V. Rodríguez, C. Janiak, G. S. Yellol, J. Ruiz, *J. Med. Chem.* **2015**, *58*, 1320-1336; d) K. Li, G. S. Ming Tong, Q. Wan, G. Cheng, W.-Y. Tong, W.-H. Ang, W.-L. Kwong, C.-M. Che, *Chem. Sci.* **2016**, *7*, 1653-1673; e) J. Sophie, E. K. Fritze, C. Angela, *Curr. Med. Chem.* **2018**, *25*, 437-461.
- [17] a) E. Lalinde, R. Lara, P. López Iciar, M. T. Moreno, E. Alfaro-Arnedo, G. Pichel José, S. Piñero-Hermida, *Chem. Eur. J.* **2018**, *24*, 2440-2456; b) M. Fereidoonzehad, Z. Ramezani, M. Nikravesh, J. Zangeneh, M. Golbon Haghghi, Z. Faghhih, B. Notash, H. R. Shahsavari, *New J. Chem.* **2018**, *42*, 7177-7187; c) M. Frezza, Q. P. Dou, Y. Xiao, H. Samouei, M. Rashidi, F. Samari, B. Hemmateenejad, *J. Med. Chem.* **2011**, *54*, 6166-6176; d) F. Samari, B. Hemmateenejad, M. Shamsipur, M. Rashidi, H. Samouei, *Inorg. Chem.* **2012**, *51*, 3454-3464.
- [18] M. Serratrice, L. Maiore, A. Zucca, S. Stoccoro, I. Landini, E. Mini, L. Massai, G. Ferraro, A. Merlino, L. Messori, M. A. Cinellu, *Dalton Trans.* **2016**, *45*, 579-590.
- [19] a) S. M. Nabavizadeh, M. Golbon Haghghi, A. R. Esmaeilbeig, F. Raoof, Z. Mandegani, S. Jamali, M. Rashidi, R. J. Puddephatt, *Organometallics* **2010**, *29*, 4893-4899; b) M. S. Sangari, M. Golbon Haghghi, S. M. Nabavizadeh, M. Kubicki, M. Rashidi, *New J. Chem.* **2017**, *41*, 13293-13302; c) R. Babadi Aghakhanpour, S. M. Nabavizadeh, M. Rashidi, *J. Organomet. Chem.* **2016**, *819*, 216-227.
- [20] C. Schmidt, B. Karge, R. Misgeld, A. Prokop, R. Franke, M. Brönstrup, I. Ott, *Chem. Eur. J.* **2017**, *23*, 1869-1880.
- [21] S. J. Berners-Price, P. J. Barnard, in *Ligand Design in Medicinal Inorganic Chemistry* (Ed.: T. Storr), John Wiley and Sons, United Kingdom, **2014**, pp. 227-256.
- [22] H. Ross, *Sirolimus and Auranofin in Treating Patients With Advanced or Recurrent Non-Small Cell Lung Cancer or Small Cell Lung Cancer*, **2019**, <https://ClinicalTrials.gov/show/NCT01737502>.
- [23] A. Jatoi, *Auranofin and Sirolimus in Treating Participants With Ovarian Cancer*, **2018**, <https://ClinicalTrials.gov/show/NCT03456700>.
- [24] V. Fernández-Moreira, M. C. Gimeno, *Chem. Eur. J.* **2018**, *24*, 3345-3353.
- [25] M.-C. Brandys, M. C. Jennings, R. J. Puddephatt, *J. Chem. Soc., Dalton Trans.* **2000**, 4601-4606.
- [26] a) A. Martín, Ú. Belío, S. Fuentès, V. Sicilia, *Eur. J. Inorg. Chem.* **2013**, *2013*, 2231-2247; b) C. Ezquerro, A. E. Sepúlveda, A. Grau-Atienza, E. Serrano, E. Lalinde, J. R. Berenguer, J. García-Martínez, *J. Mater. Chem. C* **2017**, *5*, 9721-9732.
- [27] J. R. Berenguer, E. Lalinde, M. T. Moreno, P. Montaña, *Eur. J. Inorg. Chem.* **2012**, *2012*, 3645-3654.
- [28] <http://www.webelements.com>.
- [29] N. Mirzadeh, M. A. Bennett, E. Wächter, L. Zhechkov, T. Heine, S. K. Bhargava, *J. Organomet. Chem.* **2015**, *783*, 130-134.
- [30] a) J. R. Berenguer, Á. Díez, E. Lalinde, M. T. Moreno, S. Ruiz, S. Sánchez, *Organometallics* **2011**, *30*, 5776-5792; b) M. Jamshidi, M. Babaghasabha, H. R. Shahsavari, S. M. Nabavizadeh, *Dalton Trans.* **2017**, *46*, 15919-15927; c) M. Jamshidi, S. M. Nabavizadeh, H. R. Shahsavari, M. Rashidi, *RSC Adv.* **2015**, *5*, 57581-57591.
- [31] Y. Chi, P.-T. Chou, *Chem. Soc. Rev.* **2010**, *39*, 638-655.
- [32] M. Altaf, M. Monim-ul-Mehboob, A. A. Isab, V. Dhuna, G. Bhatia, K. Dhuna, S. Altuwajiri, *New J. Chem.* **2015**, *39*, 377-385.
- [33] J. R. Berenguer, E. Lalinde, A. Martín, M. T. Moreno, S. Ruiz, S. Sánchez, H. R. Shahsavari, *Inorg. Chem.* **2014**, *53*, 8770-8785.
- [34] T. Yagyu, J.-I. Ohashi, M. Maeda, *Organometallics* **2007**, *26*, 2383-2391.

FULL PAPER

- [35] a) M. Fereidoonezhad, H. R. Shahsavari, S. Abedanzadeh, B. Behchenari, M. Hossein-Abadi, Z. Faghih, M. H. Beyzavi, *New J. Chem.* **2018**, *42*, 2385-2392; b) M. Fereidoonezhad, H. R. Shahsavari, E. Lotfi, M. Babaghasabha, M. Fakhri, Z. Faghih, Z. Faghih, M. H. Beyzavi, *Appl. Organomet. Chem.* **2018**, *32*, e4200.

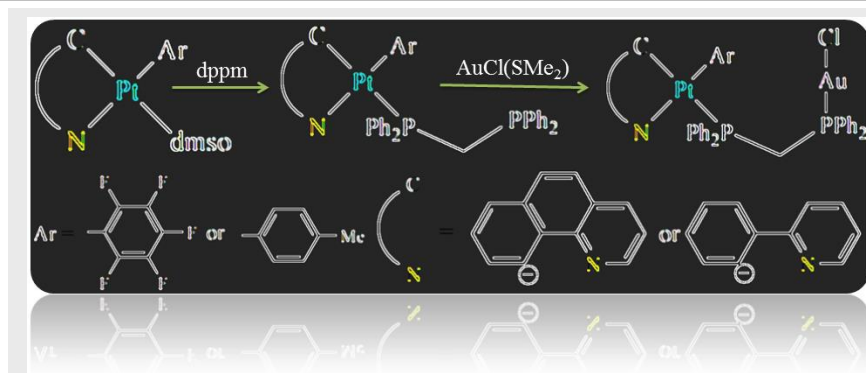
WILEY-VCH

Accepted Manuscript

FULL PAPER

Entry for the Table of Contents

FULL PAPER



Hamid R. Shamsavari*, Nora Giménez, Elena Lalinde*, M. Teresa Moreno, Masood Fereidoonzehad*, Reza Babadi Aghakhanpour, Mehri Khatami, Forough Kalantari, Zahra Jamshidi, and Mozhdeh Mohammadpour

Heterobimetallic Pt(II)-Au(I) Complexes Comprising Unsymmetrical 1,1-Bis(diphenylphosphino)methane Bridge: Synthesis, Photophysical and Cytotoxic Studies

A series of aryl-cycloplatinated(II) complexes "[Pt(C^N)(Ar)(κ¹-dppm)]" featuring dangling dppm ligand were reacted with AuCl(SMe₂) to give the heterobimetallic Pt(II)-Au(I) complexes with unsymmetrical dppm bridge. The impact of the coordination of AuCl unit on the optical properties and biological activity of the precursors has been investigated.